Music-selective neural populations arise without musical training

Dana Boebinger[1,2,3], Sam Norman-Haignere[5,6,7], Josh McDermott[1,2,3,4], Nancy Kanwisher[2,3,4]

[1] *Speech and Hearing Bioscience and Technology, Harvard University, Cambridge MA 02138 USA*
[2] *Brain and Cognitive Sciences, Massachusetts Institute of Technology, Cambridge MA 02139 USA*
[3] *McGovern Institute for Brain Research, Massachusetts Institute of Technology, Cambridge MA 02139 USA*
[4] *Center for Brains, Minds, and Machines, Massachusetts Institute of Technology, Cambridge MA 02139 USA*
[5] *HHMI Postdoctoral Fellow of the Life Sciences Research Foundation, Baltimore MD 21218 USA*
[6] *Laboratoire des Sytèmes Perceptifs, Département d'Études Cognitives, École Normale Supérieure, PSL Research University, CNRS, Paris France*
[7] *Zuckerman Institute for Brain Research, Columbia University, New York NY 10027 USA*

ABSTRACT

Recent work has shown that human auditory cortex contains neural populations anterior and posterior to primary auditory cortex that respond selectively to music. However, it is unknown how this selectivity for music arises. To test whether musical training is necessary, we measured fMRI responses to 192 natural sounds in 10 people with almost no musical training. When voxel responses were decomposed into underlying components, this group exhibited a music-selective component that was very similar in response profile and anatomical distribution to that previously seen in individuals with moderate musical training. We also found that musical genres that were less familiar to our participants (e.g., Balinese *gamelan*) produced strong responses within the music component, as did drum clips with rhythm but little melody, suggesting that these neural populations are broadly responsive to music as a whole. Our findings demonstrate that the signature properties of neural music selectivity do not require musical training to develop, demonstrating the music-selective neural populations are a fundamental and widespread property of the human brain.

Keywords: auditory cortex, decomposition, expertise, fMRI, music

Music is uniquely and universally human (Mehr et al., 2019)and musical abilities arise early in development (Trehub, 2003). Recent evidence has revealed neural populations in bilateral non-primary auditory cortex that respond selectively to music and thus seem likely to figure importantly in musical perception and behavior (Leaver and Rauschecker, 2010; Rogalsky et al., 2011; Fedorenko et al., 2012; Tierney et al., 2013; LaCroix et al., 2015; Norman-Haignere et al., 2015, 2019). How does such selectivity arise? Most members of Western societies have received at least some explicit musical training in the form of lessons or classes. However, most Western individuals, including non-musicians, also implicitly acquire knowledge of musical structure from a lifetime of exposure to music (Bigand, 1983; Bigand and Pineau, 1997; Koelsch et al., 2000; Tillmann et al., 2000; Tillmann, 2005; Bigand and Poulin-Charronnat, 2006). The roles of these two forms of musical experience in the neural representation of music are not understood. Here, we directly test whether explicit musical training is necessary for the development of music-selective neural responses, by testing whether music-selective responses are robustly present – with similar response characteristics and anatomical distribution – in individuals with little or no explicit training.

Why might explicit musical training be necessary for neural tuning to music? In animals, exposure to specific sounds can elicit long-term changes in auditory cortex, such as sharper tuning of individual neurons (Recanzone et al., 1993; Fritz et al., 2003; Lee and Middlebrooks, 2011) and expansion of cortical maps (Recanzone et al., 1993; Polley et al., 2006; Bieszczad and Weinberger, 2010). These changes occur primarily for behaviorally relevant stimulus features (Ahissar et al., 1992, 1998; Fritz et al., 2005; Ohl and Scheich, 2005; Polley et al., 2006) related to the intrinsic reward value of the stimulus (Bakin and Weinberger, 1996; Fritz et al., 2005; David et al., 2012), and thus are closely linked to the neuromodulatory system (Bao et al., 2001; Kilgard et al., 2001; Blake et al., 2006). Additionally, the extent

of cortical map expansion is correlated with the animal's subsequent improvement in behavioral performance (Recanzone et al., 1993; Rutkowski and Weinberger, 2005; Polley et al., 2006; Bieszczad and Weinberger, 2010, 2012; Reed et al., 2011). Musical training in humans meets virtually all of these criteria for eliciting functional plasticity: playing music requires focused attention, fine-grained sensory-motor coordination, and is known to engage the neuromodulatory system (Blood and Zatorre, 2001; Salimpoor et al., 2011, 2013). And expert musicians often begin training at a young age and hone their skills over many years.

Although many prior studies have measured neural responses in musicians and non-musicians (Ohnishi et al., 2001; Pantev et al., 2001; Shahin et al., 2003; Fujioka et al., 2004, 2005; Besson et al., 2007; Wong et al., 2007; Dick et al., 2011; Lee and Noppeney, 2011; Ellis et al., 2012, 2013; Angulo-Perkins et al., 2014; Doelling and Poeppel, 2015; Lappe et al., 2016), it remains unclear whether any tuning properties of auditory cortex depend on musical training. Previous studies have found that fMRI responses to music are larger in musicians compared to non-musicians in posterior superior temporal gyrus (Ohnishi et al., 2001; Dick et al., 2011; Angulo-Perkins et al., 2014). However, these responses were not shown to be selective for music, leaving the relationship between musical training and cortical music selectivity unclear.

Music selectivity is weak when measured in raw voxel responses using standard voxel-wise fMRI analyses, due to spatial overlap between music-selective neural populations and neural populations with other selectivities (e.g. pitch). To overcome these challenges, Norman-Haignere et al. (2015) used voxel decomposition to infer a small number of component response profiles that collectively explained voxel responses throughout auditory cortex to large set of natural sounds. This approach makes it possible to disentangle the responses of neural populations that overlap within voxels, and has previously revealed a neural population with clear selectivity for music compared to both other real-world sounds (Norman-Haignere et al., 2015) and synthetic control stimuli matched to music in many acoustic properties (Norman-Haignere and McDermott, 2018). These results have recently been confirmed by intracranial recordings, which show individual electrodes with clear selectivity for music (Norman-Haignere et al., 2019). Although Norman-Haignere et al. (2015) did not include actively practicing musicians, many of the participants had substantial musical training earlier in their lives.

Here, we test whether music selectivity arises only after explicit musical training. To this end, we probed for music selectivity in people with almost no musical training. If explicit musical training is necessary for the existence of music-selective neural populations, music selectivity should be weak or absent in these non-musicians. A group of highly trained musicians was also included for comparison. Using these same methods, we were also able to test whether the inferred music-selective neural population responds strongly to less familiar musical genres (e.g. Balinese *gamelan*), and to drum clips with rich rhythm but little melody.

Note that this is not a traditional group comparison study contrasting musicians and non-musicians, as it would be unrealistic to collect the amount of data that would be necessary for a direct statistical comparison between groups. Rather, our goal was to ask whether the key properties of music selectivity described in our earlier study are present in each group when analyzed separately.

MATERIALS & METHODS

Participants

Norman-Haignere et al. (2015) inferred a music-selective component from an analysis of ten participants. Although these participants were described as "non-musicians" (defined as no formal training in the five years preceding the study) many of the participants had substantial musical training earlier in life. We

therefore used stricter inclusion criteria to recruit 10 musicians and 10 non-musicians for the current study, in order to have statistical power within each group comparable to that of our previous study.

Twenty young adults (14 female, mean = 24.7 years, sd = 3.8 years) participated in the experiment: 10 non-musicians (6 female, median = 25.8 years, sd = 4.1 years) and 10 musicians (8 female, median = 23.5 years, sd = 3.3 years). To be classified as a non-musician, participants were required to have less than two years of total music training, which could not have occurred either before the age of seven or within the last five years. Out of the ten non-musicians in our sample, eight had zero years of musical training, one had a single year of musical training (at the age of 20), and one had two years of training (starting at age 10). These training measures do not include any informal "music classes" included in participants' required elementary school curriculum, because (at least in the United States) these classes are typically compulsory, are only for a small amount of time per week (e.g. 1 hour), and primarily consist of simple sing-a-longs. Inclusion criteria for musicians were beginning formal training before the age of seven (Penhune, 2011), and continuing training until the current day. Our sample of ten musicians had an average of 16.30 years of training (ranging from 11-23 years, sd = 2.52). Details of participants' musical experience can be found in **Table 1**.

	Subject #	Instrument	Age of Onset (Years)	Years of Lessons	Years of Regular Practice	Years of Training	Hours of Weekly Practice	Hours of Daily Music Listening
NON-MUSICIANS	11			0	0	0	0	0
	12		20	1	0	1	0	2
	13			0	0	0	0	0.25
	14			0	0	0	0	5
	15			0	0	0	0	1
	16			0	0	0	0	1.5
	17		10	1.5	0	1.5	0	1
	18			0	0	0	0	0.1
	19			0	0	0	0	0.5
	20			0	0	0	0	5
	mean		24.4	0.3	0	0.3	0	1.64
MUSICIANS	1	violin	7	11	11	11	2	2
	2	piano, French horn	5	7	18	12	6	4
	3	piano, bass	6	12	18	18	2	2
	4	piano	3	15	15	15	2	2.5
	5	piano, violin, viola	5	17	19	20	3	4
	6	piano, flute	5	13	13	13	12	3
	7	flute	7	12	13	15	15	3
	8	piano, cello, flute	4	19	15	18	25	1
	9	violin	3	18	18	18	4	10
	10	violin, clarinet	4	13	8	23	4	5
	mean		5.2	13.7	14.8	16.3	7.1	3.65
	grand mean		14.8	7	7.4	8.3	3.55	2.64

Table 1. Details of participants' musical backgrounds and training, as measured by a self-report questionnaire.

Non-parametric Wilcoxon rank sum tests indicated that there were no significant group differences in median age (musician median = 24.0 years, sd = 3.3, non-musician median = 25.0 years, sd = 4.1, z = -1.03, p = 0.30, effect size r = -0.23), education (musician median = 6.0 years, sd = 8.2 years, non-musician median = 6.5 years, sd = 7.5 years, z = -0.08, p = 0.94, effect size r = -0.02), or socioeconomic status as measured by the Barrett Simplified Measure of Social Status questionnaire (BSMSS; (Barratt, 2006) (musician median = 54.8, sd = 7.1, non-musician median = 53.6, sd = 15.4, z = 0.30, p = 0.76, effect size r = 0.07). All participants were native English speakers and had normal hearing (audiometric thresholds <25 dB HL for octave frequencies 250Hz to 8kHz). The study was approved by MIT's human participants review committee (COUHES), and written informed consent was obtained from all participants.

To validate participants' self-reported musicianship, we measured participants' abilities on a variety of psychoacoustical tasks for which prior evidence suggested that musicians would outperform non-musicians, including frequency discrimination, sensorimotor synchronization, melody discrimination, and "sour note" detection. As predicted, musician participants outperformed non-musician participants on all behavioral psychoacoustic tasks. See **Supplemental Information** for more details.

Study design

Each participant underwent a 2-hour behavioral testing session as well as three 2-hour fMRI scanning sessions. During the behavioral session, participants completed an audiogram, filled out questionnaires about their musical experience, and completed a series of basic psychoacoustic tasks described in **Supplemental Information**.

A. Stimulus Set of Commonly Heard Natural Sounds

1. Man speaking	11. Running water	21. Cellphone vibrating	31. Computer startup	41. Splashing water
2. Flushing toilet	12. Breathing	22. Water dripping	32. Background speech	42. Computerized speech
3. Pouring liquid	13. Keys jangling	23. Scratching	33. Songbird	43. Alarm clock
4. Tooth brushing	14. Dishes clanking	24. Car windows	34. Pouring water	44. Walking with heels
5. Woman speaking	15. Ringtone	25. Telephone ringing	35. Pop song	45. Vacuum
6. Car accelerating	16. Microwave	26. Chopping food	36. Water boiling	46. Wind
7. Biting and chewing	17. Dog barking	27. Telephone dialing	37. Guitar	47. Boy speaking
8. Laughing	18. Walking (hard surface)	28. Girl speaking	38. Coughing	48. Chair rolling
9. Typing	19. Road traffic	29. Car horn	39. Crumpling paper	49. Rock Song
10. Car engine running	20. Zipper	30. Writing	40. Siren	50. Door knocking
				…

B. Scanning Procedure and Task Structure

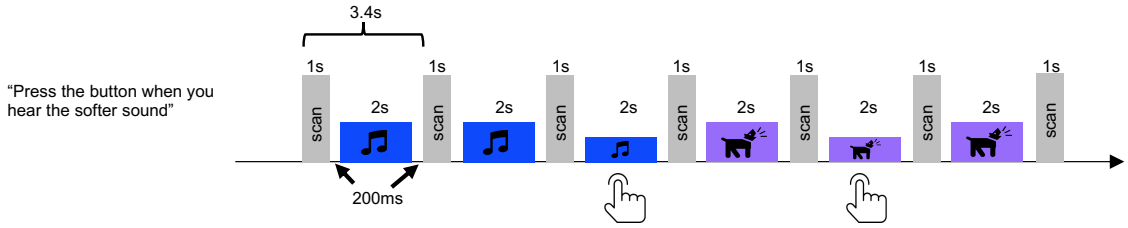

C. Voxel Decomposition Procedure

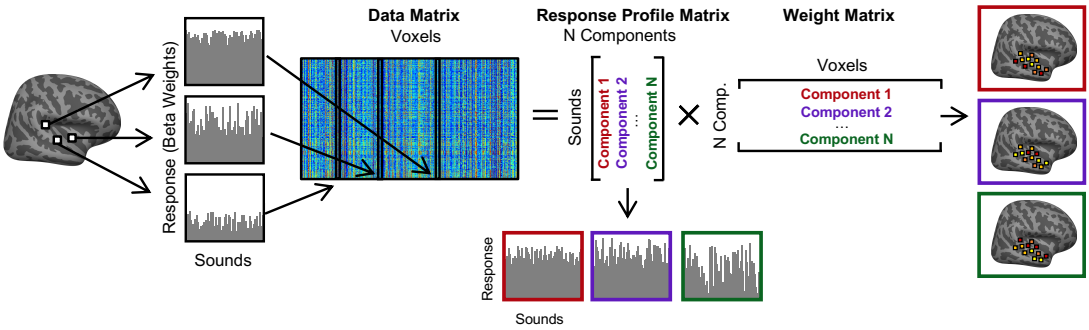

Figure 1. Experimental design and voxel decomposition method. (**A**) Fifty examples of the original set of 165 natural sounds used in Norman-Haignere et al. (2015), ordered by how often participants' reported hearing them in daily life. An additional 27 music stimuli were added to this set of 165 for the current experiment. (**B**) Scanning paradigm and task structure. Each 2-second sound stimulus was repeated three times consecutively, with one repetition (the second or third) being 12 dB quieter. Subjects were instructed to press a button when they detected this quieter sound. A sparse scanning sequence was used, in which one fMRI volume was acquired in the silent period between stimuli. (**C**) Diagram depicting the voxel decomposition method, reproduced from Norman-Haignere et al. (2015). The average response of each voxel to the 192 sounds is represented as a vector, and the response vector for every voxel from all 20 subjects is concatenated into a matrix (192 sounds x 26,792 voxels). This matrix is then factorized into a response profile matrix (192 sounds x N components) and a voxel weight matrix (N components x 26,792 voxels).

Natural sound stimuli for fMRI experiment

Stimuli consisted of 2-second clips of 192 natural sounds. These sounds included the 165-sound stimulus set used in Norman-Haignere et al. (2015), which broadly sample frequently heard and recognizable sounds from everyday life. Examples can be seen in **Figure 1A**. This stimulus set was supplemented with 27 additional music and drumming clips from a variety of musical cultures, so that we could examine responses to rhythmic features of music, as well as comparing responses to more versus less familiar musical genres. Stimuli were normalized in root mean square level (RMS = 0.1) and ramped on and off with a 25ms linear ramp. During scanning, auditory stimuli were presented over MR-compatible earphones (Sensimetrics S14) at 75 dB SPL.

An online experiment (via Amazon's Mechanical Turk) was used to assign a semantic category to each stimulus, in which 180 participants (95 females; mean age = 38.8 years, sd = 11.9 years) categorized each stimulus into one of fourteen different categories. The categories were taken from Norman-Haignere et al. (2015), with three additional categories ("non-Western instrumental music," "non-Western vocal music," "drums") added to accommodate the additional music stimuli used in this experiment.

A second Amazon Mechanical Turk experiment was run to ensure that American listeners were indeed less familiar with the non-Western music stimuli chosen for this experiment, but that they still perceived the stimuli as "music." In this experiment, 188 participants (75 females; mean age = 36.6 years, sd = 10.5 years) listened to each of the 62 music stimuli and rated them based on (1) how "musical" they sounded, (2) how "familiar" they sounded, (3) how much they "liked" the stimulus, and (4) how "foreign" they sounded.

fMRI data acquisition and preprocessing

Similar to the design of Norman-Haignere et al (2015), sounds were presented during scanning in a "mini-block design," in which each 2-second natural sound was repeated three times in a row. Sounds were repeated because we have found this makes it easier to detect reliable hemodynamic signals. We used fewer repetitions than in our prior study (3 vs. 5), because we wanted to test a larger number of sounds and because we observed similarly reliable responses using fewer repetitions in pilot experiments. Each stimulus was presented in silence, with a single fMRI volume collected between each repetition (i.e. "sparse scanning," (Hall et al., 1999)). To encourage participants to pay attention to the sounds, either the second or third repetition in each "mini-block" was 12dB quieter (presented at 67 dB SPL), and participants were instructed to press a button when they heard this quieter sound (**Figure 1B**). Overall, participants performed well on this task (musicians: mean = 92.06%, sd = 5.47%; non-musicians: mean = 91.47%, sd = 5.83%; no participant's average performance across runs fell below 80%). Each of the three scanning sessions consisted of sixteen 5.5-minute runs, for a total of 48 functional runs per participant. Each run consisted of 24 stimulus mini-blocks and five silent blocks during which no sounds were presented. These silent blocks were the same duration as the stimulus mini-blocks, and were distributed evenly throughout each run, providing a baseline. Each specific stimulus was presented in two mini-blocks per scanning session, for a total of six mini-block repetitions per stimulus over the three scanning sessions. Stimulus order was randomly permuted across runs and across participants.

MRI data were collected at the Athinoula A. Martinos Imaging Center of the McGovern Institute for Brain Research at MIT, on a 3T Siemens Prisma with a 32-channel head coil. Each volume acquisition lasted 1 second, and the 2-second stimuli were presented during periods of silence between each acquisition, with a 200ms buffer of silence before and after stimulus presentation. As a consequence, one brain volume was collected every 3.4 seconds (1 second + 2 seconds + 0.2*2 seconds) (TR = 3.4s, TA = 1.02s, TE = 33ms, 90 degree flip angle, 4 discarded initial acquisitions). Each functional acquisition consisted of 48 roughly axial slices (oriented parallel to the anterior-posterior commissure line) covering the whole brain, each slice being 3mm thick and having an in-plane resolution of 2.1 x 2.1mm (96 x 96 matrix, 0.3mm slice gap). An SMS acceleration factor of 4 was used in order to minimize acquisition time (TA =

1.02s). To localize functional activity, a high-resolution anatomical T1-weighted image was obtained for every participant (TR = 2.53 seconds, voxel size: 1mm^3, 176 slices, 256 x 256 matrix).

Preprocessing and data analysis were performed using FSL software and custom Matlab scripts. Functional volumes were motion-corrected, slice-time-corrected, skull-stripped, linearly detrended, and aligned to each participant's anatomical image (using FLIRT and BBRegister; (Jenkinson and Smith, 2001; Greve and Fischl, 2009). Motion correction and function-to-anatomical registration was done separately for each run. Preprocessed data were then resampled to the cortical surface reconstruction computed by FreeSurfer (Dale et al., 1999), and smoothed on the surface using a 3mm FWHM kernel to improve SNR. The data were then downsampled to a 2mm isotropic grid on the FreeSurfer-flattened cortical surface.

Next, we estimated the response to each of the 192 stimuli using a general linear model (GLM). Each stimulus mini-block was modeled as a boxcar function convolved with a canonical hemodynamic response function (HRF). The model also included six motion regressors and a first-order polynomial noise regressor to account for linear drift in the baseline signal. Note that this analysis differs from our prior paper (Norman-Haignere et al., 2015), in which signal averaging was used in place of a GLM. We made this change because BOLD responses were estimated more reliably using an HRF-based GLM, potentially due to the use of shorter stimulus blocks causing more overlap between BOLD responses to different stimuli.

Voxel selection

The first step of this analysis method is to determine which voxels serve as input to the decomposition algorithm. All analyses were carried out on voxels within a large anatomical constraint region encompassing bilateral superior temporal and posterior parietal cortex (**Supplemental Figure 1**), as in Norman-Haignere et al. (2015). In practice, the vast majority of voxels with a robust and reliable response to sound fell within this region (**Supplemental Figure 2**), which explains why our results were very similar with and without this anatomical constraint (**Supplemental Figure 3**). Within this large anatomical region, we selected voxels that displayed a significant ($p < 0.001$, uncorrected) response to sound (pooling over all sounds compared to silence). This consisted of 51.45% of the total number of voxels within our large constraint region. We also selected only voxels that produced a reliable response pattern to the stimuli across scanning sessions. Note that rather than using a simple correlation to determine reliability, we used the equation from Norman-Haignere et al. (2015) to measure the reliability across split halves of our data. This reliability measure differs from a Pearson correlation in that it assigns high values to voxels that respond consistently to sounds and does not penalize them even if their response does not vary much between sounds, which is the case for many voxels within primary auditory cortex:

$$r = 1 - \frac{\| \boldsymbol{v}_1 - proj_{\boldsymbol{v}_2}\boldsymbol{v}_1 \|^2}{\| \boldsymbol{v}_1 \|^2}$$

$$proj_{\boldsymbol{v}_2}\boldsymbol{v}_1 = \boldsymbol{v}_2 \left(\frac{\boldsymbol{v}_2{}^T}{\| \boldsymbol{v}_2 \|^2} \boldsymbol{v}_1 \right)$$

where $\boldsymbol{v}_1$ and $\boldsymbol{v}_2$ indicate the vector of beta weights from a single voxel for the 192 sounds, estimated separately for the two halves of the data ($\boldsymbol{v}_1$ = first three repetitions from runs 1-24, $\boldsymbol{v}_2$ = last three repetitions from runs 25-48), and $\| \|$ is the L2 norm. Note that these equations differ from Equations 1 and 2 in Norman-Haignere et al. (2015), because the equations reported previously contained an error: the L2-norm terms were not squared. We used the same reliability cutoff as in our prior study ($r > 0.3$). Of the sound-responsive voxels, 54.47% of them also met the reliability criteria. Using these two selection

criteria, the median number of voxels per participant = 1,286, sd = 254 (**Supplemental Figure 1A**). The number of selected voxels did not differ significantly between musicians (median = 1,216, sd = 200) and non-musicians (medians = 1,341, sd = 284; z = -1.40, p = 0.16, effect size r = -0.31, two-tailed Wilcoxon rank sum test), and the anatomical location of the selected voxels was largely similar across groups (**Supplemental Figure 1B**).

Unlike our prior study, we collected whole-brain data in this experiment and thus were able to repeat our analyses without any anatomical constraint. While a few additional voxels outside of the mask do meet our selection criteria (**Supplemental Figure 2**), the resulting components are very similar to those obtained using the anatomical mask, both in response profiles (**Supplemental Figure 3A**; correlations ranging from r = 0.91 to r > 0.99, sd = 0.03) and voxel weights (**Supplemental Figure 3B**).

Decomposition algorithm

The decomposition algorithm approximates the response of each voxel ($\boldsymbol{v}_i$) as the weighted sum of a small number of component response profiles that are shared across voxels (**Figure 1B**):

$$\boldsymbol{v}_i \approx \sum_{k=1}^{K} \boldsymbol{r}_k w_{k,i}$$

where $\boldsymbol{r}_k$ represents the kth component response profile that is shared across all voxels, $w_{k,i}$ represents the weight of component k in voxel i, and K is the total number of components.

We concatenated the selected voxel responses from all participants into a single data matrix $\boldsymbol{D}$ (S sounds $\times$ V voxels). We then approximated the data matrix as the product of two smaller matrices: (1) a response matrix $\boldsymbol{R}$ (S sounds x K components) containing the response profile of all inferred components to the sound set, and (2) a weight matrix $\boldsymbol{W}$ (K components $\times$ V voxels) containing the contribution of each component response profile to each voxel. Using matrix notation this yields:

$$\boldsymbol{D} \approx \boldsymbol{RW}$$

The method used to infer components was described in detail in our prior paper (Norman-Haignere et al., 2015) and code is available online (https://github.com/snormanhaignere/nonparametric-ica). The method is similar to standard algorithms for independent components analysis (ICA) in that it searches amongst the many possible solutions to the factorization problem for components that have a maximally non-Gaussian distribution of weights across voxels (the non-Gaussianity of the components inferred in this study can be seen in **Supplemental Figure 4**). The method differs from most standard ICA algorithms in that it does so by directly minimizing the entropy of the component weight distributions across voxels as measured by a histogram, which is feasible due to the large number of voxels. Entropy is a natural measure to minimize because the Gaussian distribution has maximal entropy. The algorithm achieves this goal in two steps. First, PCA is used to whiten and reduce the dimensionality of the data matrix. This was implemented using the singular value decomposition:

$$\boldsymbol{D} \approx \boldsymbol{U}^k \boldsymbol{S}^k \boldsymbol{V}^k$$

where $\boldsymbol{U}^k$ contains the response profiles of the top K principal components (192 sounds $\times$ K components), $\boldsymbol{V}^k$ contains the whitened voxel weights for these components (K components $\times$ 26,792 voxels), and $\boldsymbol{S}^k$ is a diagonal matrix of singular values ($K \times K$). The number of components (K) was chosen by measuring the amount of voxel response variance explained by different numbers of components and the accuracy of the components in predicting voxel responses in left-out data. Specifically, we chose a value of K that balanced these two measures such that the set of components

explained a large fraction of the voxel response variance (which increases monotonically with additional components), but still maintained good prediction accuracy (which decreases once additional components begin to cause overfitting). In practice, the plateau in the amount of explained variance coincided with the peak of the prediction accuracy.

The principal component weight matrix is then rotated to maximize the negentropy (*J*) summed across components:

$$\widehat{\boldsymbol{T}} = \underset{\boldsymbol{T}}{\operatorname{argmax}} \sum_{c=1}^{N} J(\boldsymbol{W}[c,:]), \quad \text{where } \boldsymbol{W} = \boldsymbol{T}\boldsymbol{V}^{k}$$

where $\boldsymbol{W}$ is the rotated weight matrix ($K \times 26{,}792$), $\boldsymbol{T}$ is an orthonormal rotation matrix ($K \times K$), and $\boldsymbol{W}[c,:]$ is the cth row of $\boldsymbol{W}$. We estimated entropy using a histogram-based method (Moddemeijer, 1989) applied to the voxel weight vector for each component ($\boldsymbol{W}[c,:]$), and defined negentropy as the difference in entropy between the empirical weight distribution and a Gaussian distribution of the same mean and variance:

$$J(\boldsymbol{y}) = H(\boldsymbol{y}_{gauss}) - H(\boldsymbol{y})$$

The optimization is performed by iteratively rotating pairs of components to maximize negentropy, which is a simple algorithm that does not require the computation of gradients, and is feasible for small numbers of components (the number of component pairs grows as $\binom{K}{2}$).

We carried out this voxel decomposition analysis on three different data sets: i) on voxels from the 10 musicians only, ii) on voxels from the 10 non-musicians only, and iii) on voxels from all twenty participants.

Measuring component selectivity

To quantify the selectivity of the music component, we measured the difference in mean response profile magnitude between music and non-music sounds, divided by their pooled standard deviation (Cohen's d). This measure provides a measure of the separability of the two sound categories within the response profile. We measured Cohen's d for several different pairwise comparisons of sound categories. In each case, the significance of the separation of the two stimulus categories was determined using a permutation test (permuting stimulus labels between the two categories 10,000 times). This null distribution was then fit with a Gaussian, a p-value from which was assigned to the observed value of Cohen's d.

Anatomical component weight maps

To visualize the anatomical distribution of component weights, individual participants' component weights were projected onto the cortical surface of the standard Freesurfer FsAverage template, and a random effects analysis (t-test) was performed to determine whether component weights were significantly greater than zero across participants at each voxel. To visualize the component weight maps separately for musicians and non-musicians, a separate random effects analysis was run for the participants in each group. To correct for multiple comparisons, we adjusted the false discovery rate (FDR, c(V) = 1, q = 0.05) using the method from Genovese, Lazar, and Nichols (Genovese et al., 2002).

Component voxel weights within anatomical ROIs

In addition to projecting the weight distributions on the cortical surface, we summarized their anatomical distribution by measuring the mean component voxel weight within a set of standardized anatomical parcels (Glasser et al., 2016). These mean weights were computed separately for each participant, and then averaged across participants for visualization purposes (e.g. **Figure 5B**). We then ran a 4 (ROI) x 2

(hemisphere) repeated-measures ANOVA on these weights. A separate ANOVA was run for musicians and non-musicians, to evaluate each group separately.

To compare the magnitude of the main effect of ROI with the main effect of hemisphere, we bootstrapped across participants, resampling participants 1,000 times. We re-ran the repeated-measures ANOVA on each sample, each time measuring the difference in the effect size for the two main effects, i.e. η_{pROI}^2 - η_{pHemi}^2. We then calculated the 95% CI of this distribution of effect size differences. The significance of the difference in main effects was evaluated by determining whether or not each group's 95% CI for the difference overlapped with zero.

In addition, we ran a Bayesian repeated-measures ANOVA on these same data, implemented in JASP v.0.13.1, using the default prior (Cauchy distribution, r = 0.5). Effects are reported as the Bayes Factor for inclusion (BF_{inc}) of each main effect and/or interaction, which is the ratio between the likelihood of the data given the model including the effect in question vs. the likelihood of the next simpler model without the effect in question.

RESULTS

Our primary question was whether cortical music selectivity is present in people with almost no musical training. To that end, we scanned ten people with almost no musical training (**Table 1**), and used voxel decomposition to isolate music-selective neural populations. We also included another set of ten participants with extensive musical training for comparison. First, we asked whether the response components across all of auditory cortex reported by Norman-Haignere et al. (2015) replicate in both non-musicians and highly trained musicians when analyzed separately. Second, we examined the detailed characteristics of music selectivity in particular, to test whether its previously documented key properties are present in both non-musicians and highly trained musicians. Third, we took advantage of our expanded stimulus set to look at additional properties of music selectivity, such as the response to musical genres that are less familiar to our Western participants.

Replication of functional components of auditory cortex from Norman-Haignere et al. (2015) in musicians and in non-musicians

Replication of previous voxel decomposition results

We first tested the extent to which we would replicate the overall functional organization of auditory cortex reported by Norman-Haignere et al. (2015) in people with almost no musical training, using the voxel decomposition method introduced in that paper. We also performed the same analysis on a group of highly trained musicians. Specifically, in every participant, we measured the response of voxels within auditory cortex to 192 natural sounds (**Figure 1A** & **B;** the average response of each voxel to each sound was estimated using a standard hemodynamic response function). These 192 sounds included the 165 sounds used in the original study along with additional music clips to further explore brain responses to foreign music and drumming. Then, separately for non-musicians and musicians, we used voxel decomposition to model the response of these voxels as the weighted sum of a small number of canonical response components (**Figure 1C**). This method factorizes the voxel responses into two matrices: one containing the components' response profiles across the sound set, and the second containing voxel weights specifying the extent to which each component contributes to the response of each voxel. The method searches for components that have maximally non-Gaussian weight distributions (**Supplemental Figure 4**). The logic of this approach is that independent non-Gaussian variables become more Gaussian when they are linearly mixed, and thus non-Gaussianity provides a statistical signature that can be used to detect the unmixed components. Similar to standard algorithms for independent components analysis

(ICA), the method maximizes non-Gaussianity by minimizing entropy, since the Gaussian distribution is maximally entropic.

Since the only free parameter in this analysis is the number of components recovered, the optimal number of components was determined by measuring the fraction of the reliable response variance the components explain. In the previous study (Norman-Haignere et al., 2015), six components were sufficient to explain over 80% of the reliable variance in voxel responses. We found the same to be true in both participant groups of the current study: six components were needed to optimally model the data from the 10 participants in separate analyses of each group. The six components explained 88.56% and 88.09% of the reliable voxel response variance for non-musicians and musicians respectively, after which the amount of explained variance for each additional component plateaued (**Supplemental Figure 5**).

Next, we examined the similarity of the components inferred from non-musicians to the components from our previous study, comparing their responses to the 165 sounds common to both experiments. Because the order of the components inferred using ICA holds no significance, we first used the Hungarian algorithm (Kuhn, 1955) to optimally reorder the components, maximizing their correlation with the components from our previous study. For comparisons of the response profile matrices of two groups of subjects, we matched components using the weight matrices; conversely, for comparisons involving the voxel weights, we matched components using the response profile matrices (see Methods). In practice, the component matches were identical regardless of which matrices were used for matching. We also conducted the same analysis for the musicians, comparing the components derived from their data to those in our previous study.

For both non-musicians and musicians, corresponding pairs of components were highly correlated with those from our previous study, with r-values for non-musicians' components ranging from 0.63 to 0.99 (**Figure 2A** & **B**) and from 0.66 to 0.99 for musicians' components (**Figure 2C** & **D**).

<u>Component response profiles and selectivity for sound categories</u>

Four of the six components from our previous study captured expected acoustic properties of the sound set (e.g. frequency, spectrotemporal modulation; see **Supplemental Figure 6A** for analyses relating the responses of these components to audio frequency and spectrotemporal modulation) and were

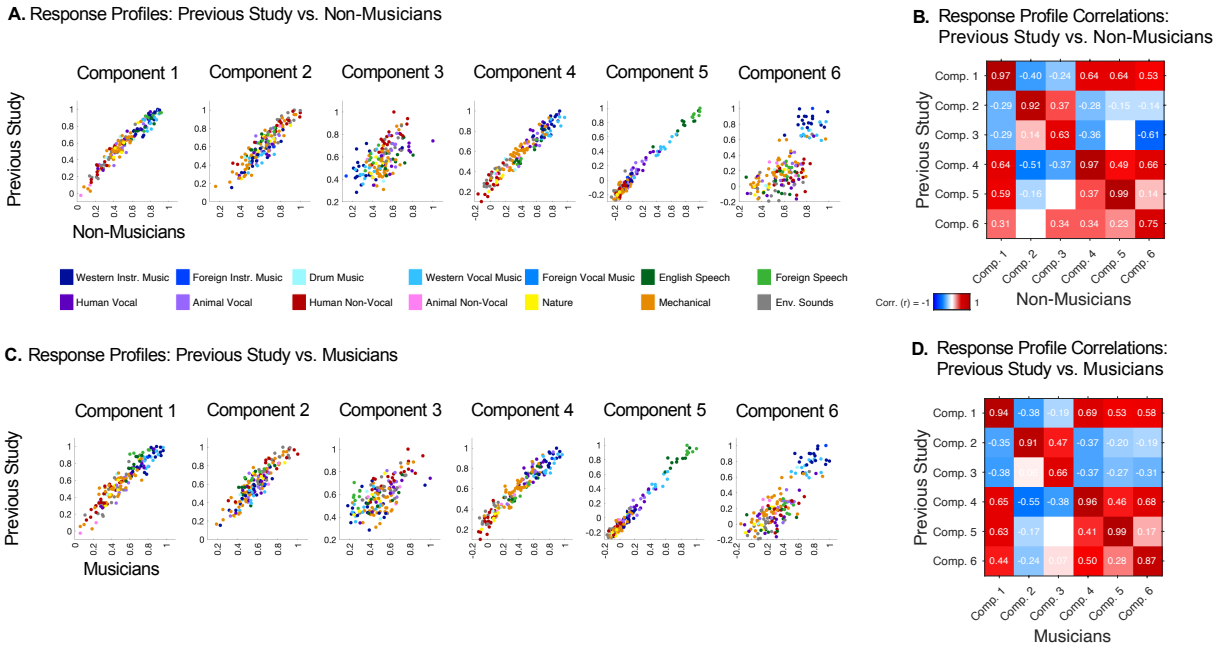

Figure 2. Replication of components from Norman-Haignere et al. (2015). (**A**) Scatterplots showing the correspondence between the component response profiles from the previous study (y-axis) and those inferred from non-musicians (x-axis). Sounds are colored according to their semantic category, as determined by raters on Amazon Mechanical Turk. Note that the axes differ slightly between groups in order to make it possible to clearly compare the pattern of responses across sounds independent of the overall response magnitude. (**B**) Correlation matrix comparing component response profiles from the previous study (y-axis) and those inferred from non-musicians (x-axis). (**C, D**) Same as **A & B** but for musicians.

concentrated in and around primary auditory cortex (PAC), consistent with prior results (Chi et al., 2005; Schönwiesner and Zatorre, 2009; Humphries et al., 2010; Da Costa et al., 2011; Herdener et al., 2013; Santoro et al., 2014; Hullett et al., 2016; Norman-Haignere and McDermott, 2018). The two remaining components responded selectively to speech (**Figure 3A**, left column) and music (**Figure 3B**, left column), respectively, and were not well accounted for using acoustic properties alone (**Supplemental Figure 6A**). The corresponding components inferred from non-musicians (**Figure 3A** & **B**, middle columns) and musicians (**Figure 3A** & **B**, right columns) also show this category selectivity.

We also found similarities in the anatomical distribution of speech- and music-selective component weights between the previous study and both groups in the current study. The weights for the speech-selective component were concentrated in the middle portion of the superior temporal gyrus (midSTG, **Figure 3C**), as expected based on previous reports (Scott et al., 2000; Hickok and Poeppel, 2007; Overath et al., 2015). In contrast, the weights for the music-selective component were most prominent anterior to PAC in the planum polare, with a secondary cluster posterior to PAC in the planum temporale (**Figure 3D**) (Ohnishi et al., 2001; Margulis et al., 2009; Dick et al., 2011; Fedorenko et al., 2012; Angulo-Perkins et al., 2014; Armony et al., 2015; Norman-Haignere et al., 2015).

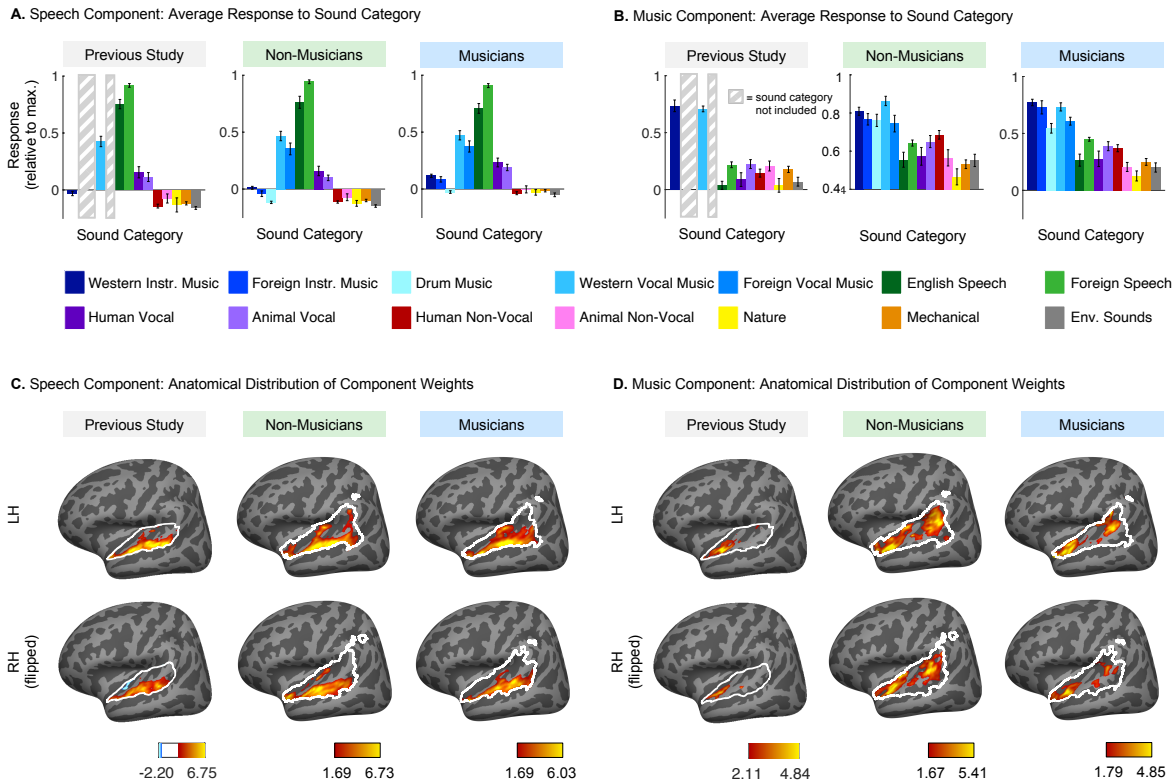

Figure 3. Comparison of speech-selective and music-selective components for participants from previous study, non-musicians, and musicians. Component response profiles averaged by sound category (as determined by raters on Amazon Mechanical Turk). (**A**) The speech-selective component responds highly to speech and music with vocals, and minimally to all other sound categories. Shown separately for the previous study (left), non-musicians (middle) and musicians (right). Note that the previous study contained only a subset of the stimuli used in the current study, so some conditions were not included and are thus replaced by a gray rectangle. (**B**) The music-selective component (right) responds highly to both instrumental and vocal music, and less strongly to other sound categories. Note that "Western Vocal Music" stimuli were sung in English. Note the different axis limits for the two groups to accommodate different 'DC' offsets. For both **A** and **B**, error bars plot one standard error of the mean across sounds from a category, computed using bootstrapping (10,000 samples). (**C**) Spatial distribution of speech-selective component voxel weights in both hemispheres. (**D**) Spatial distribution of music-selective component voxel weights. Color denotes the statistical significance of the weights, computed using a random effects analysis across subjects comparing weights against 0; p values are logarithmically transformed ($-\log_{10}[p]$). The white outline indicates the voxels that were both sound-responsive (sound vs. silence, $p < 0.001$ uncorrected) and split-half reliable ($r > 0.3$) at the group level (see Methods for details). The color scale represents voxels that are significant at FDR $q = 0.05$, with this threshold computed for each component separately. Voxels that do not survive FDR correction are not colored, and these values appear as white on the color bar. The right hemisphere (bottom rows) is flipped to make it easier to visually compare weight distributions across hemispheres.

Together, these findings show that we are able to twice replicate the overall component structure underlying of auditory cortical responses described in our previous study (once for non-musicians and once for musicians). Further, both non-musicians and musicians show the same category-selective components as in our previous study, including a single component that appears to be selective for music.

Characterizing music selectivity in non-musicians and musicians separately

We next asked whether nonmusicians exhibited the signature response characteristics of music selectivity documented in our prior paper: (1) the music component response profile showed a high response to both instrumental and vocal music and a low response to all other categories, including

speech, (2) music component voxel weights were high in anterior and posterior superior temporal gyrus (STG), and low in both PAC and lateral STG, and (3) music component voxel weights had a largely bilateral distribution. We examined whether each of these properties was present in the components separately inferred from non-musicians and musicians.

Response profiles show selectivity for both instrumental and vocal music

The defining feature of the music-selective component from Norman-Haignere et al. (2015) was that its response profile showed a very high response to stimuli that had been categorized by humans as "music", including both instrumental music and music with vocals, relative to non-music stimuli, including speech (**Figure 3B**, left column). The category-averaged responses of the music-selective component showed similar effects in non-musicians and highly trained musicians (**Figure 3B**, center and right columns).

To quantify this music selectivity, we measured the difference in mean response profile magnitude between music and non-music sounds, divided by their pooled standard deviation (Cohen's d). So that we could compare across our previous and current experiments, this was done using the set of 165 sounds that were common to both studies. We measured Cohen's d separately for several different pairwise comparisons: (1) instrumental music vs. speech stimuli, (2) instrumental music vs. other non-music stimuli, (3) vocal music vs. speech stimuli, and (4) vocal music vs. other non-music stimuli (**Figure 4**). In each case, the significance of the separation of the two stimulus categories was determined using a nonparametric test permuting stimulus labels 10,000 times. All four of these statistical comparisons were highly significant for non-musicians when analyzed separately (all p's < 10^{-5}, **Table 2**). This result shows that the music component is highly music selective in non-musicians, in that it responds highly to both instrumental and vocal music, and significantly less to both speech and other non-music sounds. Similar results were also found for musicians (all p's < 10^{-5}, **Table 2**).

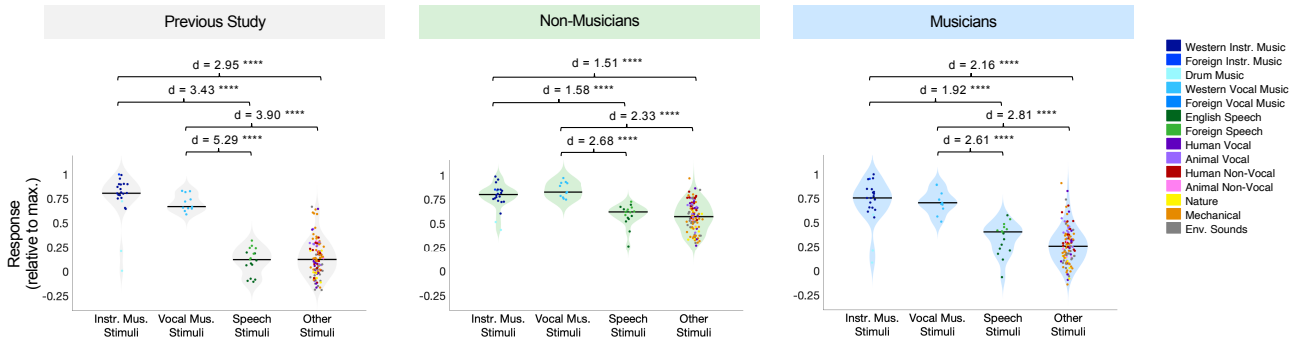

Figure 4. Separability of sound categories in music-selective components of non-musicians and musicians. Distributions of (1) instrumental music stimuli, (2) vocal music stimuli, (3) speech stimuli, and (4) other stimuli within the music component response profiles from our previous study (left, grey shading), as well as those inferred from musicians (center, blue shading) and non-musicians (right, green shading). The mean for each stimulus category is indicated by the horizontal black line. The separability between pairs of stimulus categories (as measured using Cohen's d) is shown above each plot. Individual sounds are colored according to their semantic category. See **Table 2** for results of pairwise comparisons indicated by brackets; **** = significant at p < 0.0001 two-tailed.

We note that the mean response profile magnitude for the music-selective component differed between groups, being lower in musicians than non-musicians (note different axes in **Figure 3B**). However this effect is unlikely to be a consequence of musical training because mean response magnitude was lower still in the previous study, whose participants had substantially less musical training than the musicians in the current study.

		Stimulus Category	Mean	SD	Cohen's d	p-value
NON-MUSICIANS	1	Instrumental Music	0.78	0.13	1.58	2.14e-06
		Speech	0.59	0.11		
	2	Instrumental Music	0.78	0.13	1.51	1.88e-10
		Other	0.57	0.15		
	3	Vocal Music	0.85	0.08	2.68	4.54e-11
		Speech	0.59	0.11		
	4	Vocal Music	0.85	0.08	2.33	1.87e-12
		Other	0.57	0.15		
MUSICIANS	1	Instrumental Music	0.72	0.22	1.92	1.19e-08
		Speech	0.34	0.16		
	2	Instrumental Music	0.72	0.22	2.16	7.40e-20
		Other	0.27	0.19		
	3	Vocal Music	0.72	0.12	2.61	8.38e-11
		Speech	0.34	0.16		
	4	Vocal Music	0.72	0.12	2.81	3.62e-18
		Other	0.27	0.19		

Table 2. Results of pairwise comparisons between stimulus categories shown in **Figure 4B**. The significance of the separation of the two stimulus categories was determined using a nonparametric test permuting stimulus labels 10,000 times.

Music component weights concentrated in anterior and posterior STG

A second notable property of the music component from Norman-Haignere et al. (2015) was that the weights were concentrated in distinct regions of non-primary auditory cortex, with prominent clusters in anterior and posterior STG. Conversely, music component weights were low in primary auditory cortex (PAC) and non-primary lateral STG.

To assess whether these anatomical characteristics were evident for the music components inferred from our non-musician and musician participants, we superimposed standardized anatomical parcels (Glasser et al., 2016) on the data, and defined anatomical regions of interest (ROIs) by selecting four sets of these anatomically-defined parcels corresponding to anterior non-primary, primary, and lateral

non-primary auditory cortex (**Figure 5A**). We then calculated the average music component weight for each individual participant within each of these four anatomical ROIs, separately for each hemisphere (**Figure 5B**). This was done separately for non-musicians and musicians, using their respective music

components. We did not perform this analysis on the data from our previous study because its anatomical coverage was more restricted than the data we collected here.

For each group, a 4 (ROI) x 2 (hemisphere) repeated measures ANOVA on these mean component weights showed a significant main effect of ROI for both non-musicians ($F(3, 27) = 50.51$, $p = 3.32e\text{-}11$, $\eta_p^2 = 0.85$) and musicians ($F(3, 27) = 20.00$, $p = 4.98e\text{-}07$, $\eta_p^2 = 0.70$). Planned pairwise comparisons showed that for each group, component weights were significantly higher in the anterior and posterior non-primary ROIs than both the primary and lateral non-primary ROIs when averaging over hemispheres (**Table 3**; non-musicians: all p's < 0.003, musicians: all p's < 0.02,).

These results show that in both non-musicians and musicians, music selectivity is concentrated in anterior and posterior STG, and present to a lesser degree in lateral STG, and only minimally in PAC.

<u>Music component weights are bilaterally distributed</u>

A third characteristic of the previously described music selectivity is that it was similarly distributed across hemispheres, with no obvious lateralization (Norman-Haignere et al., 2015). The repeated-measures ANOVA described above showed no evidence of lateralization in either non-musicians or musicians (**Figure 5B**; non-musicians: $F(1, 9) = 0.02$, $p = 0.91$, $\eta_p^2 = 0.001$; musicians: $F(1, 9) = 1.55$, $p = 0.24$, $\eta_p^2 = 0.15$). Furthermore, for both groups, the effect size of ROI within a hemisphere was significantly larger than the effect size of hemisphere (measured by bootstrapping across participants to get 95% CIs around the difference in the effect size for the two main effects, i.e. $\eta_{pROI}^2 - \eta_{pHemi}^2$; the significance of the difference in main effects was evaluated by determining

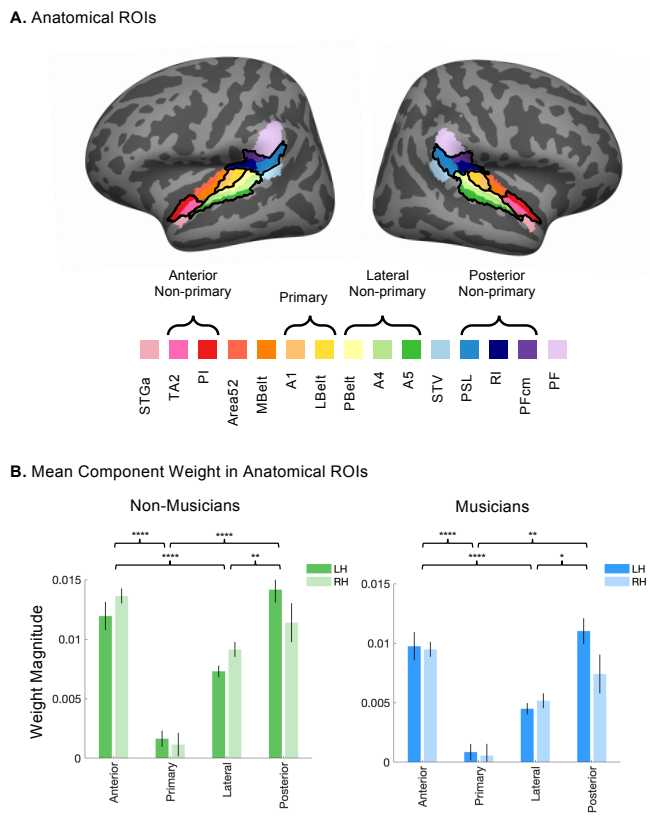

Figure 5. Quantification of bilateral anterior/posterior concentration of voxel weights for the music-selective components inferred in non-musicians and musicians separately. (A) Fifteen standardized anatomical parcels were selected from Glasser et al. (2016), chosen to fully encompass the superior temporal plane and superior temporal gyrus (STG). To come up with a small set of ROIs to use to evaluate the music component weights in our current study, we superimposed these anatomical parcels onto the weights of the music component from our previously published study (Norman-Haignere et al., 2015), and then defined ROIs by selecting sets of the anatomically-defined parcels that correspond to regions of high (anterior non-primary, posterior non-primary) vs. low (primary, lateral non-primary) music component weights. The anatomical parcels that comprise these four ROIs are indicated by the brackets, and outlined in black on the cortical surface. (B) Mean music component weight across all voxels in each of the four anatomical ROIs, separately for each hemisphere, and separately for non-musicians (left, green shading) and musicians (right, blue shading) and A repeated-measures ROI x hemisphere ANOVA was conducted for each group separately. Error bars plot one standard error of the mean across participants. Brackets represent pairwise comparisons that were conducted between ROIs with expected high vs. low component weights, averaged over hemisphere. See **Table 3** for full results of pairwise comparisons, and **Supplemental Figure 7** for component weights from all fifteen anatomical parcels. * = significant at $p < 0.05$ two-tailed, ** = significant at $p < 0.01$ two-tailed, *** = significant at $p < 0.001$ two-tailed, **** = significant at $p < 0.0001$ two-tailed. Note that because our prior hypotheses required that all four of these pairwise contrasts be significant, there is no need to correct for multiple comparisons.

Table 3. Results of pairwise comparisons between mean weights in ROIs shown in **Figure 5B**. Component weights were first averaged over hemispheres and significance between ROI pairs was evaluated using paired t-tests. Note that because our strict criteria required that all four of these pairwise contrasts be significant, there is no need to correct for multiple comparisons.

Subject Group	ROI		t-Value	Cohen's d	p-value
Non-musicians	1 Anterior non-primary	2 Primary	15.00	6.04	3.44e-08
	1 Anterior non-primary	3 Lateral non-primary	8.74	2.84	1.08e-05
	1 Anterior non-primary	4 Posterior non-primary	7.34	2.29	4.98e-05
	2 Primary	3 Lateral non-primary	3.95	1.31	0.0031
	2 Primary	4 Posterior non-primary	11.45	3.84	1.12e-06
	3 Lateral non-primary	4 Posterior non-primary	7.72	2.42	2.94e-05
Musicians	1 Anterior non-primary	2 Primary	13.00	4.54	1.42	0.0014
	1 Anterior non-primary	3 Lateral non-primary	7.47	2.36	6.06e-05
	1 Anterior non-primary	4 Posterior non-primary	2.29	0.72	0.0304
	2 Primary	3 Lateral non-primary	3.81	1.20	0.0034
	2 Primary	4 Posterior non-primary	7.72	2.42	2.94e-05
	3 Lateral non-primary	4 Posterior non-primary	4.54	1.42	0.0014

whether or not each group's 95% CI for the difference overlapped with zero: non-musicians' CI = [0.38 0.90], musicians' CI = [0.05 0.81]).

We note that both groups showed a significant ROI x hemisphere interaction (non-musicians: $F(3, 27) = 4.04$, $p = 0.02$, $\eta_p^2 = 0.31$; musicians: $F(3, 27) = 4.45$, $p = 0.01$, $\eta_p^2 = 0.15$;). However, a Bayesian repeated-measures ANOVA provided no evidence for an ROI x hemisphere interaction. We used JASP (JASP Team, 2020), using its default prior (Cauchy distribution, r = 0.5), and computed the Bayes Factor for inclusion of each main effect and/or interaction (the ratio between the likelihood of the data given the model including the effect in question vs. the likelihood of the next simpler model without the effect in question). The Bayes Factor for the interaction between ROI and hemisphere were close to 1 (BF_{incl} for non-musicians = 1.65, BF_{incl} for musicians = 0.51). There was also either no evidence for a main effect of hemisphere (BF_{incl} for musicians = 0.45) or evidence against it (BF_{incl} for non-musicians = 0.23). By contrast, the main effect of ROI was well supported (Bayes factor of inclusion, BF_{incl}, for ROI for non-musicians = 1.39e17, and for musicians = 1.62e10). So while we cannot exclude the possibility of some differences between music selectivity in the two hemispheres, or that such differences might interact with musical training, any such hemispheric differences appear modest relative to the pronounced ROI differences within hemisphere, as these were by far the dominant effect for both groups.

The fact that the music component inferred from non-musicians exhibits all of the previously described features of music selectivity (Norman-Haignere et al., 2015) suggests that explicit musical training is not necessary for a music-selective neural population to arise in the human brain. In addition, the results from musicians suggest that that the signature properties of music selectivity are not drastically altered by extensive musical experience. Both groups exhibited a single response component selective for music. And in both groups, this selectivity was present for both instrumental and vocal music, was localized to anterior and posterior non-primary auditory cortex, and was present bilaterally.

New insights into music selectivity: Music-selective regions of auditory cortex show high responses to drum rhythms and unfamiliar musical genres

Because our experiment utilized a broader stimulus set than the original study (Norman-Haignere et al., 2015), we were able to use the inferred components to ask additional questions about the effect of experience on music selectivity, as well as gain new insights into the nature of cortical music selectivity. The set of natural sounds used in this study included a total of 62 music stimuli, spanning a variety of instruments, genres, and cultures. Using this diverse set of music stimuli, we can begin to address the questions of (1) whether music selectivity is specific to the music of one's own culture, and (2) whether music selectivity is driven solely by features related to pitch, like the presence of a melody. Here we analyze the music component inferred from all 20 participants since similar music components were inferred separately from musicians and non-musicians (see **Supplemental Figure 8** for details of the components inferred from all 20 participants).

To expand beyond the original stimulus set from Norman-Haignere et al. (2015), which contained music exclusively from traditionally Western genres and artists, we selected additional music clips from several non-Western musical cultures that varied in tonality and rhythmic complexity (e.g. Indian raga, Balinese gamelan, Chinese opera, Mongolian throat singing, Jewish klezmer, Ugandan lamellophone music) (**Figure 6A**). We expected that our American participants would have less exposure to these musical genres, allowing us to see whether the music component makes a distinction between familiar and less familiar music. The non-Western music stimuli were rated by American Mechanical Turk participants as being similarly musical (mean rating on 1-100 scale for Western music = 86.28, sd = 7.06; Non-Western music mean = 79.63, sd = 9.01; $p = 0.37$, 10,000 permutations) but less familiar (mean rating on 1-100 scale for Western music = 66.50, sd = 8.23; Non-Western music mean = 45.50, sd = 15.83; $p < 1.0e-5$, 10,000 permutations) than typical Western music. Despite this difference in familiarity, the magnitude of

non-Western music stimuli within the music component was only slightly smaller than the magnitude of Western music stimuli (Cohen's d = 0.64), a difference that was only marginally significant (**Figure 6B**; p = 0.052, nonparametric test permuting music stimulus labels 10,000 times). Moreover, the magnitudes of both Western and non-Western music stimuli were both much higher than non-music stimuli (Western music stimuli vs. non-music stimuli: Cohen's d = 3.79, p < 0.0001, 10,000 permutations; non-Western music vs. non-music: Cohen's d = 2.85; p < 0.0001, 10,000 permutations). Taken together, these results suggest that music-selective responses in auditory cortex occur even for relatively unfamiliar musical systems and genres.

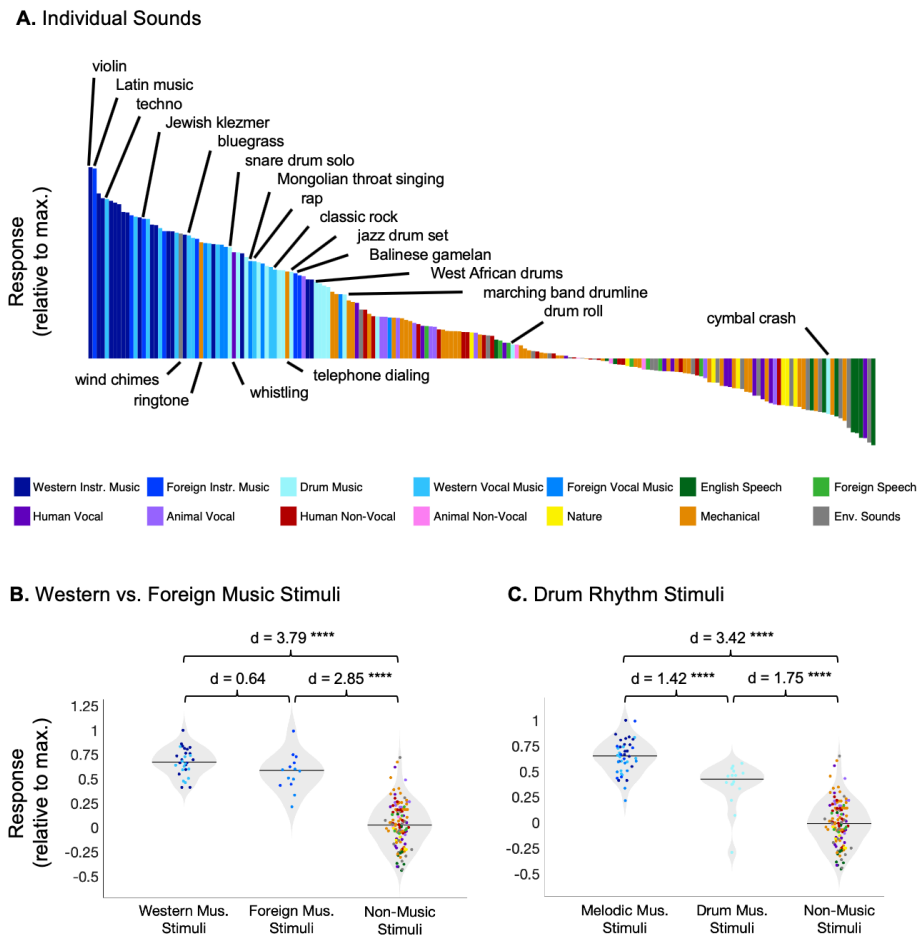

Figure 6. (**A**) Close-up of the response profile (192 sounds) for the music component inferred from all participants (n = 20), with example stimuli labeled. Note that there are a few "non-music" stimuli (categorized as such by Amazon Mechanical Turk raters) with high component rankings, but that these are all arguably musical in nature (e.g. wind chimes, ringtone). Conversely, "music" stimuli with low component rankings (e.g. "drumroll" and "cymbal crash") do not contain salient melody or rhythm, despite being classified as "music" by human listeners. (**B**) Distributions of Western music stimuli (left), non-Western music stimuli (middle), and non-music stimuli (right) within the music component response profile inferred from all 20 participants, with the mean for each stimulus group indicated by the horizontal black line. The separability between categories of stimuli (as measured using Cohen's d) is shown above the plot. Note that drum stimuli were left out of this analysis. (**C**) Distributions of melodic music stimuli (left), drum rhythm stimuli (middle), and non-music stimuli (right) within the music component response profile inferred from all 20 participants, with the mean for each stimulus group indicated by the horizontal black line. The separability between categories of stimuli (as measured using Cohen's d) is shown above the plot. Sounds are colored according to their semantic category. **** = significant at p < 0.0001 two-tailed.

Which stimulus features drive music selectivity? One of the most obvious distinctions is between melody and rhythm. While music typically involves both melody and rhythm, when assembling our music stimuli

we made an attempt to pick clips that varied in the prominence and complexity of their melodic and rhythmic content. In particular, we included 13 stimuli consisting of drumming from a variety of genres and cultures, because drum music mostly isolates the rhythmic features of music while minimizing (though not eliminating) melodic features. Whether music-selective auditory cortex would respond highly to these drum stimuli was largely unknown, partially because the Norman-Haignere et al. (2015) study only included two drum stimuli, one of which was just a stationary snare drum roll that produced a low response in the music component, likely because it lacks both musical rhythm and pitch structure. However, the drum stimuli in our study ranked relatively high in the music component response profile, averaging only slightly below the other instrumental and vocal music category responses (Cohen's $d = 1.42$, $p < 8.76e\text{-}07$), and considerably higher than the other non-music stimulus categories (Cohen's $d = 1.75$, $p < 9.60e\text{-}11$) (**Figure 6C**). This finding suggests that the music component is not simply tuned to melodic information, but is also sensitive to rhythm.

DISCUSSION

Our results show that cortical music selectivity is present in non-musicians and hence does not require explicit musical training to develop. Indeed, the same six response components that characterized human auditory cortical responses to natural sounds in our previous study were replicated twice here, once in non-musicians, and once in musicians. Our goal in this study was not to make statistical comparisons between non-musicians and musicians (which would have required a prohibitive amount of data) but rather to assess whether the key properties of music selectivity were present in each group. Indeed, in both groups, voxel decomposition produced a single music-selective component, which was selective for both instrumental and vocal music, and was concentrated bilaterally in anterior and posterior superior temporal gyrus (STG). We also observed that the music-selective component responds strongly to both drums and less familiar non-Western music. Together, these results show that passive exposure to music is sufficient for the development of music selectivity in non-primary auditory cortex, and that music-selective responses extend to rhythms with little melody, and to relatively unfamiliar musical genres.

Origins of music selectivity

Our finding of music-selective responses in non-musicians suggests that music selectivity is either present from birth or results from passive exposure to music. If present from birth, music selectivity could in principle represent an evolutionary adaptation for music, definitive evidence for which has long been elusive (Darwin, 1871). But it is also plausible that music-specific representations emerge over development from the common presence of music in human environments. For example, optimizing a neural network model to solve ecological speech and music tasks yields separate processing streams for the two tasks (Kell et al., 2018), suggesting that musical tasks sometimes require music-specific features. Music-specific features might also emerge in humans or machines without tasks per se. Music is acoustically distinct from other natural sounds, and generic unsupervised learning, for instance for producing efficient representations of sound (Lewicki, 2002; Carlson et al., 2012; Młynarski and McDermott, 2019), might produce a set of features that are activated primarily by musical sounds.

Nearly all of our participants reported listening to music on a daily basis, and in other contexts this everyday musical experience has clear effects (Bigand, 1983; Bigand and Pineau, 1997; Koelsch et al., 2000; Tillmann et al., 2000; Tillmann, 2005; Bigand and Poulin-Charronnat, 2006), providing an example of how unsupervised learning from music might alter representations in the brain. For instance, behavioral studies of non-industrialized societies who lack much contact with Western culture show pronounced differences from Westerners in many aspects of music perception (McDermott et al., 2016; Jacoby and McDermott, 2017; Jacoby et al., 2019; McPherson et al., 2020). Thus, our data do not show that music selectivity in the brain is independent of experience. Indeed, it is possible that the brains of people who grow up with less extensive musical exposure than our participants would not display such pronounced

music selectivity. Rather, these results show that typical exposure to music in Western culture is sufficient for cortical music selectivity to emerge.

What does cortical music selectivity represent?

The music-selective component responds strongly to a wide range of music and weakly to virtually all other sounds, demonstrating that it is driven by a set of features that are relatively specific to music. One possibility is that there are simple acoustic features that differentiate music from other types of stimuli. Speech and music are known to differ in their temporal modulation spectra, peaking at 5 Hz and 2 Hz, respectively (Ding et al., 2017), and some theories suggest that these acoustic differences lead to neural specialization for speech vs. music in different cortical regions (Albouy et al., 2020). However, standard auditory models based on spectrotemporal modulation do not capture the perception of speech and music (McDermott and Simoncelli, 2011) or neural responses selective for speech and music (Overath et al., 2015; Kell et al., 2018; Norman-Haignere and McDermott, 2018; Zuk et al., 2020). In particular, the music-selective component responds substantially less to sounds that have been synthesized to have the same spectrotemporal modulation statistics as natural music, suggesting that the music component does not simply represent the audio or modulation frequencies that are prevalent in music (Norman-Haignere and McDermott, 2018).

Our finding that the music-selective component shows high responses to less familiar musical genres places some constraints on what these properties might be, as does the short duration of the stimuli used to characterize music selectivity. For instance, the music-specific features that drive the response are unlikely to be specific to Western music, and must unfold over relatively short timeframes. Features that are common to nearly all music, but not other types of sounds, include stable and sustained pitch organized into discrete note-like elements, and temporal patterning with regular time intervals. Because the music component anatomically overlaps with more general responses to pitch (Norman-Haignere et al., 2015), it is natural to wonder if it represents higher-order aspects of pitch, such as the above-mentioned stability, or discrete jumps from one note to another. However, the high response to drum rhythms in the music component that we observed here indicates that the component is not only sensitive to pitch structure. Instead, this result suggests that melody and rhythm might be jointly analyzed, rather than dissociated, at least at the level of auditory cortex. One possibility is that the underlying neural circuits extract temporally local representations of melody and rhythm motifs that are assembled elsewhere into the representations of contour, key, meter, groove etc. that are the basis of music cognition (Janata et al., 2002; Brett and Grahn, 2007; Lee et al., 2011; Fedorenko et al., 2012; Matthews et al., 2020).

Limitations

Our paradigm used relatively brief stimuli since music-selective regions are present just outside of primary auditory cortex, where integration periods appear to be short (Overath et al., 2015). And we used an intentionally simple task (intensity discrimination) in order to encourage subjects to generically attend to all stimuli. It is thus possible that more complex stimuli or tasks would reveal additional aspects of music-selective responses, that might not be present to a similar degree in non-musicians. One relevant point of comparison is the finding that amusic participants with striking pitch perception deficits show pitch-selective auditory cortical responses that are indistinguishable from those of control participants with univariate analyses (Norman-Haignere et al., 2016). Recent evidence suggests it is nonetheless possible to discriminate amusic participants from controls, and to predict participants' behavioral performance, using fMRI data collected in the context of a pitch task (Albouy et al., 2019). Utilizing a music-related task might produce larger differences between musicians and non-musicians, as might longer music stimuli (compared to the 2-second clips used in this experiment), which could be argued to contain richer melodic, harmonic, and/or rhythmic information.

Finally, our study is limited by the resolution of fMRI. Voxel decomposition is intended to help overcome the spatial limitations of fMRI, and indeed appears to reveal responses that are not evident in raw voxel responses but can be seen with finer-grained measurement substrates such as electrocorticography (Norman-Haignere et al., 2019). But the spatial and temporal resolution of the BOLD signal inevitably constrain what is detectable, which likely explains why we have only been able to detect six reliable response components across all of auditory cortex. Music-selective brain responses might well exhibit additional characteristics that would only be evident in fine-grained spatial and temporal patterns that cannot be resolved with fMRI, and if so, it is possible that some of these patterns would be absent or altered in non-musicians.

Future directions

One of the most interesting open questions raised by our findings is whether cortical music selectivity reflects implicit knowledge gained through typical exposure to music, or whether it is present from birth. These hypotheses could be addressed by testing people with very different musical experiences from non-Western cultures or other populations whose lifetime perceptual experience with music is limited in some way (e.g., people with musical anhedonia, children of deaf adults). It would also be informative to test whether music selectivity is present in infants or young children. Finally, much remains to be learned about the nature of cortical music selectivity, such as what acoustic or structural features might be driving it. The voxel decomposition approach provides one way of answering these questions and exploring the quintessentially human ability for music.

ACKNOWLEDGEMENTS
This work was supported by NSF grant BCS-1634050 to J.M. and NIH grant DP1HD091947 to N.K. The Athinoula A. Martinos Imaging Center at MIT is supported by the NIH Shared instrumentation grant #S10OD021569. Thank you to the McDermott lab for useful comments on an earlier version of this manuscript.

REFERENCES

Ahissar E, Abeles M, Ahissar M, Haidarliu S, Vaadia E (1998) Hebbian-like functional plasticity in the auditory cortex of the behaving monkey. Neuropharmacology 37:633–655.

Ahissar E, Vaadia E, Ahissar M, Bergman H, Arieli A, Abeles M (1992) Dependence of cortical plasticity on correlated activity of single neurons and on behavioral context. Science 257:1412–1415.

Albouy P, Benjamin L, Morillon B, Zatorre RJ (2020) Distinct sensitivity to spectrotemporal modulation supports brain asymmetry for speech and melody. Science 367.

Albouy P, Caclin A, Norman-Haignere S V., Lévêque Y, Peretz I, Tillmann B, Zatorre RJ (2019) Decoding task-related functional brain imaging data to identify developmental disorders: The case of congenital amusia. Frontiers in Neuroscience 13:1–13.

Allison PD (1978) Measures of Inequality. American Sociological Review 43:865–880.

Alluri V, Brattico E, Toiviainen P, Burunat I, Bogert B, Numminen J, Kliuchko M (2015) Musical expertise modulates functional connectivity of limbic regions during continuous music listening. Psychomusicology: Music, Mind, and Brain 25:443–454.

Angulo-Perkins A, Aubé W, Peretz I, Barrios FA, Armony JL, Concha L (2014) Music listening engages specific cortical regions within the temporal lobes: Differences between musicians and non-musicians. Cortex 59:126–137.

JASP Team (2020) JASP (Version 0.13.1).

Armony JL, Aubé W, Angulo-Perkins A, Peretz I, Concha L (2015) The specificity of neural responses to music and their relation to voice processing: An fMRI-adaptation study. Neuroscience Letters 593:35–39.

Bailey JA, Penhune VB (2010) Rhythm synchronization performance and auditory working memory in early- and late-trained musicians. Experimental Brain Research 204:91–101.

Bakin JS, Weinberger NM (1996) Induction of a physiological memory in the cerebral cortex by stimulation of the nucleus basalis. Proceedings of the National Academy of Sciences of the United States of America 93:11219–11224.

Bao S, Chan VT, Merzenich MM (2001) Cortical remodelling induced by activity of ventral tegmental dopamine neurons. Nature 412:92–95.

Barratt W (2006) The Barratt simplified measure of social status (BSMSS). Terre Haute, IN: Indiana State University.

Bashwiner DM, Wertz CJ, Flores RA, Jung RE (2016) Musical Creativity “Revealed” in Brain Structure: Interplay between Motor, Default Mode, and Limbic Networks. Scientific Reports 6:1–8.

Baumann S, Koeneke S, Schmidt CF, Meyer M, Lutz K, Jancke L (2007) A network for audio-motor coordination in skilled pianists and non-musicians. Brain Research 1161:65–78.

Baumann S, Petkov CI, Griffiths TD (2013) A unified framework for the organisation of the primate auditory cortex. Frontiers in Systems Neuroscience 7:1–19.

Bermudez P, Lerch JP, Evans AC, Zatorre RJ (2009) Neuroanatomical correlates of musicianship as revealed by cortical thickness and voxel-based morphometry. Cerebral Cortex 19:1583–1596.

Besson M, Schön D, Moreno S, Santos A, Magne C (2007) Influence of musical expertise and musical training on pitch processing in music and language. Restorative neurology and neuroscience 25:399–410.

Bieszczad KM, Weinberger NM (2010) Learning strategy trumps motivational level in determining learning-induced auditory cortical plasticity. Neurobiology of Learning and Memory 93:229–239.

Bieszczad KM, Weinberger NM (2012) Extinction reveals that primary sensory cortex predicts reinforcement outcome. European Journal of Neuroscience 35:598–613.

Bigand E (1983) Perceiving Musical Stability: The Effect of Tonal Structure, Rhythm, and Musical Expertise. Journal of Experimental Psychology: Human Perception and Performance 23:808–822.

Bigand E, Pineau M (1997) Global context effects on musical expectancy. Perception & Psychophysics 59:1098–1107.

Bigand E, Poulin-Charronnat B (2006) Are we “experienced listeners”? A review of the musical capacities that do not depend on formal musical training. Cognition 100:100–130.

Blake DT, Heiser MA, Caywood M, Merzenich MM (2006) Experience-Dependent Adult Cortical Plasticity Requires Cognitive Association between Sensation and Reward. Neuron 52:371–381.

Blood AJ, Zatorre RJ (2001) Intensely pleasurable responses to music correlate with activity in brain regions implicated in reward and emotion. Proceedings of the National Academy of Sciences of the United States of America 98:11818–11823.

Brainard DH (1997) The Psychophysics Toolbox. Spatial Vision 10:433–436.

Brett M, Grahn JA (2007) Rhythm and beat perception in motor areas of the brain. Journal of Cognitive Neuroscience 19:893–906.

Carlson NL, Ming VL, DeWeese MR (2012) Sparse codes for speech predict spectrotemporal receptive fields in the inferior colliculus. PLoS Computational Biology 8.

Chen JL, Penhune VB, Zatorre RJ (2008) Moving on Time: Brain Network for Auditory–Motor Synchronization is Modulated by Rhythm Complexity and Musical Training. Journal of Cognitive Neuroscience 20:226–239.

Chi T, Ru P, Shamma SA (2005) Multiresolution spectrotemporal analysis of complex sounds. The Journal of the Acoustical Society of America 1181:887–906.

Da Costa S, Van Der Zwaag W, Marques JP, Frackowiak RSJ, Clarke S, Saenz M (2011) Human Primary Auditory Cortex Follows the Shape of Heschl's Gyrus. The Journal of Neuroscience 31:14067–14075.

Dale AM, Fischl B, Sereno MI (1999) Cortical surface-based analysis: I. Segmentation and surface reconstruction. NeuroImage 9:179–194.

Darwin C (1871) The descent of man and selection in relation to sex. London: John Murray.

David S V., Fritz JB, Shamma SA (2012) Task reward structure shapes rapid receptive field plasticity in auditory cortex. Proceedings of the National Academy of Sciences of the United States of America 109:2144–2149.

de Aquino MPB, Verdejo-Román J, Pérez-García M, Pérez-García P (2019) Different role of the supplementary motor area and the insula between musicians and non-musicians in a controlled musical creativity task. Scientific Reports 9:1–13.

de Manzano Ö, Ullén F (2017) Same Genes, Different Brains: Neuroanatomical Differences Between Monozygotic Twins Discordant for Musical Training. Cerebral Cortex:1–8.

Dick F, Ling Lee H, Nusbaum H, Price CJ (2011) Auditory-Motor Expertise Alters "'Speech Selectivity'" in Professional Musicians and Actors. Cerebral Cortex 21:938–948.

Ding N, Patel AD, Chen L, Butler H, Luo C, Poeppel D (2017) Temporal modulations in speech and music. Neuroscience and Biobehavioral Reviews 81:181–187.

Doelling KB, Poeppel D (2015) Cortical entrainment to music and its modulation by expertise. Proceedings of the National Academy of Sciences 112:E6233-42.

Elbert T, Pantev C, Wienbruch C, Rockstroh B, Taub E (1995) Increased cortical representation of the fingers of the left hand in string players. Science 270:305–307.

Ellis RJ, Bruijn B, Norton AC, Winner E, Schlaug G (2013) Training-mediated leftward asymmetries during music processing: A cross-sectional and longitudinal fMRI analysis. NeuroImage 75:97–107.

Ellis RJ, Norton AC, Overy K, Winner E, Alsop DC, Schlaug G (2012) Differentiating maturational and training influences on fMRI activation during music processing. NeuroImage 60:1902–1912.

Fedorenko E, McDermott JH, Norman-Haignere S V., Kanwisher NG (2012) Sensitivity to musical structure in the human brain. Journal of Neurophysiology 108:3289–3300.

Foster NE V., Zatorre RJ (2010) Cortical structure predicts success in performing musical transformation judgments. NeuroImage 53:26–36.

Fritz J, Elhilali M, Shamma S (2005) Active listening: Task-dependent plasticity of spectrotemporal receptive fields in primary auditory cortex. Hearing Research 206:159–176.

Fritz J, Shamma S, Elhilali M, Klein D (2003) Rapid task-related plasticity of spectrotemporal receptive fields in primary auditory cortex. Nature Neuroscience 6:1216–1223.

Fujioka T, Trainor LJ, Ross B, Kakigi R, Pantev C (2004) Musical training enhances automatic encoding of melodic contour and interval structure. Journal of Cognitive Neuroscience 16:1010–1021.

Fujioka T, Trainor LJ, Ross B, Kakigi R, Pantev C (2005) Automatic encoding of polyphonic melodies in musicians and nonmusicians. Journal of Cognitive Neuroscience 17:1578–1592.

Gaser C, Schlaug G (2003) Grey Matter Differences between Musicians and Nonmusicians. Annals of the New York Academy of Sciences 999:514–517.

Genovese CR, Lazar NA, Nichols T (2002) Thresholding of statistical maps in functional neuroimaging using the false discovery rate. NeuroImage 15:870–878.

Glasser MF, Coalson TS, Robinson EC, Hacker CD, Harwell J, Yacoub E, Ugurbil K, Andersson J, Beckmann CF, Jenkinson M, Smith SM, Van Essen DC (2016) A multi-modal parcellation of human cerebral cortex. Nature 536:171–178.

Grahn JA, Rowe JB (2009) Feeling the Beat: Premotor and Striatal Interactions in Musicians and Nonmusicians during Beat Perception. Journal of Neuroscience 29:7540–7548.

Greve DN, Fischl B (2009) Accurate and robust brain image alignment using boundary-based registration. NeuroImage 48:63–72.

Hall DA, Haggard MP, Akeroyd MA, Palmer AR, Summerfield AQ, Elliott MR, Gurney EM, Bowtell RW (1999) “Sparse” temporal sampling in auditory fMRI. Human Brain Mapping 7:213–223.

Halwani GF, Loui P, Rüber T, Schlaug G (2011) Effects of practice and experience on the arcuate fasciculus: comparing singers, instrumentalists, and non-musicians. Frontiers in Psychology 2:156.

Hamilton LS, Edwards E, Chang EF (2018) A Spatial Map of Onset and Sustained Responses to Speech in the Human Superior Temporal Gyrus. Current Biology 28:1860–1871.

Harris R, De Jong BM (2015) Differential parietal and temporal contributions to music perception in improvising and score-dependent musicians, an fMRI study. Brain Research 1624:253–264.

Herdener M, Esposito F, Scheffler K, Schneider P, Logothetis NK, Uludag K, Kayser C (2013) Spatial representations of temporal and spectral sound cues in human auditory cortex ScienceDirect. Cortex 49:2822–2833.

Hickok G, Poeppel D (2007) The cortical organization of speech processing. Nature reviews Neuroscience 8:393–402.

Hullett PW, Hamilton LS, Mesgarani N, Schreiner CE, Chang EF (2016) Human Superior Temporal Gyrus Organization of Spectrotemporal Modulation Tuning Derived from Speech Stimuli. Journal of Neuroscience 36:2014–2026.

Humphries C, Liebenthal E, Binder JR (2010) Tonotopic organization of human auditory cortex. NeuroImage 50:1202–1211.

Imfeld A, Oechslin MS, Meyer M, Loenneker T, Jancke L (2009) White matter plasticity in the corticospinal tract of musicians : A diffusion tensor imaging study. NeuroImage 46:600–607.

Jacoby N, McDermott JH (2017) Integer Ratio Priors on Musical Rhythm Revealed Cross-culturally by Iterated Reproduction. Current Biology 27:359–370.

Jacoby N, Undurraga EA, McPherson MJ, Valdés J, Ossandón T, McDermott JH (2019) Universal and Non-universal Features of Musical Pitch Perception Revealed by Singing. Current Biology 29:3229–3243.

Janata P, Birk JL, Van Horn JD, Leman M, Tillmann B, Bharucha JJ (2002) The cortical topography of tonal structures underlying western music. Science 298:2167–2170.

Janata P, Grafton ST (2003) Swinging in the brain: Shared neural substrates for behaviors related to sequencing and music. Nature Neuroscience 6:682–687.

Jenkinson M, Smith S (2001) A global optimisation method for robust affine registration of brain images. Medical Image Analysis 5:143–156.

Kell AJE, Yamins DLK, Shook EN, Norman-Haignere S V., McDermott JH (2018) A Task-Optimized Neural Network Replicates Human Auditory Behavior, Predicts Brain Responses, and Reveals a Cortical Processing Hierarchy. Neuron 98:630-644.e16.

Kilgard MP, Pandya PK, Vazquez J, Gehi A, Schreiner CE, Merzenich MM (2001) Sensory input directs spatial and temporal plasticity in primary auditory cortex. Journal of Neurophysiology 86:326–338.

Kishon-Rabin L, Amir O, Vexler Y, Zaltz Y (2001) Pitch discrimination: Are professional musicians better than non-musicians? Journal of Basic and Clinical Physiology and Pharmacology 12:125–144.

Koelsch S, Gunter T, Friederici AD, Èger ES (2000) Brain Indices of Music Processing: "Nonmusicians'' are Musical. Journal of Cognitive Neuroscience 12:520–541.

Kuhn HW (1955) The Hungarian Method for the Assignment Problem. Naval Research Logistics Quarterly 2:83–97.

LaCroix AN, Diaz AF, Rogalsky C (2015) The relationship between the neural computations for speech and music perception is context-dependent: an activation likelihood estimate study. Frontiers in Psychology 6:1–19.

Lappe C, Lappe M, Pantev C (2016) Differential processing of melodic, rhythmic and simple tone deviations in musicians -an MEG study. NeuroImage 124:898–905.

Leaver AM, Rauschecker JP (2010) Cortical representation of natural complex sounds: effects of acoustic features and auditory object category. The Journal of Neuroscience 30:7604–7612.

Lee CC, Middlebrooks JC (2011) Auditory cortex spatial sensitivity sharpens during task performance. Nature Neuroscience 14:108–116.

Lee H, Noppeney U (2011) Long-term music training tunes how the brain temporally binds signals from multiple senses. Proceedings of the National Academy of Sciences 108.

Lee YS, Janata P, Frost C, Hanke M, Granger R (2011) Investigation of melodic contour processing in the brain using multivariate pattern-based fMRI. NeuroImage 57:293–300.

Levitt H (1971) Transformed Up-Down Methods in Psychoacoustics. The Journal of the Acoustical Society of America 49:467–477.

Lewicki MS (2002) Efficient coding of natural sounds. Nature Neuroscience 5:356–363.

Luo C, Guo Z wei, Lai Y xiu, Liao W, Liu Q, Kendrick KM, Yao D zhong, Li H (2012) Musical training induces functional plasticity in perceptual and motor networks: Insights from resting-state fMRI. PLoS ONE 7:1–10.

Margulis EH, Mlsna LM, Uppunda AK, Parrish TB, Wong PCM (2009) Selective neurophysiologic responses to music in instrumentalists with different listening biographies. Human Brain Mapping 30:267–275.

Matthews TE, Witek MAG, Lund T, Vuust P, Penhune VB (2020) The sensation of groove engages motor and reward networks. NeuroImage 214:116768.

McDermott JH, Keebler M V., Micheyl C, Oxenham AJ (2010) Musical intervals and relative pitch: Frequency resolution, not interval resolution, is special. The Journal of the Acoustical Society of America 128:1943–1951.

McDermott JH, Schultz AF, Undurraga EA, Godoy RA (2016) Indifference to dissonance in native Amazonians reveals cultural variation in music perception. Nature 535:547–550.

McDermott JH, Simoncelli EP (2011) Sound Texture Perception via Statistics of the Auditory Periphery: Evidence from Sound Synthesis. Neuron 71:926–940.

McPherson MJ, Dolan SE, Durango A, Ossandon T, Valdés J, Undurraga EA, Jacoby N, Godoy RA, McDermott JH (2020) Perceptual fusion of musical notes by native Amazonians suggests universal representations of musical intervals. Nature Communications 11:1–14.

McPherson MJ, McDermott JH (2018) Diversity in pitch perception revealed by task dependence. Nature Human Behaviour 2:52–66.

Mehr SA, Singh M, Knox D, Ketter DM, Pickens-jones D, Atwood S, Lucas C, Egner A, Jacoby N, Hopkins EJ, Howard M, Donnell TJO, Pinker S, Krasnow MM, Glowacki L (2019) Universality and diversity in human song. Science 366.

Micheyl C, Delhommeau K, Perrot X, Oxenham AJ (2006) Influence of musical and psychoacoustical training on pitch discrimination. Hearing Research 219:36–47.

Młynarski W, McDermott JH (2019) Ecological origins of perceptual grouping principles in the auditory system. Proceedings of the National Academy of Sciences of the United States of America 116:25355–25364.

Moddemeijer R (1989) On estimation of entropy and mutual information of continuous distributions. Signal Processing 16:233–248.

Nieto-Castañón A, Fedorenko EG (2012) Subject-specific functional localizers increase sensitivity and functional resolution of multi-subject analyses. NeuroImage 63:1646–1669.

Norman-Haignere S V., Albouy P, Caclin A, McDermott JH, Kanwisher NG, Tillmann B (2016) Pitch-Responsive Cortical Regions in Congenital Amusia. Journal of Neuroscience 36:2986–2994.

Norman-Haignere S V., Feather J, Brunner P, Ritaccio A, McDermott JH, Schalk G, Kanwisher NG (2019) Intracranial recordings from human auditory cortex reveal a neural population selective for musical song. bioRxiv.

Norman-Haignere S V., Kanwisher NG, McDermott JH (2013) Cortical pitch regions in humans respond primarily to resolved harmonics and are located in specific tonotopic regions of anterior auditory cortex. Journal of Neuroscience 33:19451–19469.

Norman-Haignere S V., Kanwisher NG, McDermott JH (2015) Distinct Cortical Pathways for Music and Speech Revealed by Hypothesis-Free Voxel Decomposition. Neuron 88:1281–1296.

Norman-Haignere S V., McDermott JH (2018) Neural responses to natural and model-matched stimuli reveal distinct computations in primary and nonprimary auditory cortex. PLoS Biology 16.

Ohl FW, Scheich H (2005) Learning-induced plasticity in animal and human auditory cortex. Current Opinion in Neurobiology 15:470–477.

Ohnishi T, Matsuda H, Asada T, Aruga M, Hirakata M, Nishikawa M, Katoh A, Imabayashi E (2001) Functional Anatomy of Musical Perception in Musicians. Cerebral Cortex 11:754–760.

Overath T, Mcdermott JH, Zarate JM, Poeppel D (2015) The cortical analysis of speech-specific temporal structure revealed by responses to sound quilts. Nature Neuroscience 18:903–911.

Pantev C, Larry Roberts CE, Schulz M, Engelien A, Ross B (2001) Timbre-specific enhancement of auditory cortical representations in musicians. NeuroReport 12:959–4965.

Patterson RD, Uppenkamp S, Johnsrude IS, Griffiths TD (2002) The processing of temporal pitch and melody information in auditory cortex. Neuron 36:767–776.

Penagos H, Melcher JR, Oxenham AJ (2004) A neural representation of pitch salience in nonprimary human auditory cortex revealed with functional magnetic resonance imaging. Journal of Neuroscience 24:6810–6815.

Penhune VB (2011) Sensitive periods in human development: evidence from musical training. Cortex 47:1126–1137.

Polak R, Jacoby N, Fischinger T, Goldberg D, Holzapfel A, London J (2018) Rhythmic prototypes across cultures: A comparative study of tapping synchronization. Music Perception 36:1–23.

Polley DB, Steinberg EE, Merzenich MM (2006) Perceptual Learning Directs Auditory Cortical Map Reorganization through Top-Down Influences. Journal of Neuroscience 26:4970–4982.

Puschmann S, Baillet S, Zatorre RJ (2018) Musicians at the Cocktail Party: Neural Substrates of Musical Training During Selective Listening in Multispeaker Situations. Cerebral Cortex:1–13.

Rauschecker JP, Tian B, Hauser M (1995) Processing of Complex Sounds in the Macaque Nonprimary Auditory Cortex. Science 268:111–114.

Recanzone GG, Schreiner CE, Merzenich MM (1993) Plasticity in the Frequency Representation of Primary Auditory Cortex following Discrimination Training in Adult Owl Monkeys. The Journal of Neuroscience 13:87–103.

Reed A, Riley J, Carraway R, Carrasco A, Perez C, Jakkamsetti V, Kilgard MP (2011) Cortical Map Plasticity Improves Learning but Is Not Necessary for Improved Performance. Neuron 70:121–131.

Repp BH (2005) Sensorimotor synchronization: A review of the tapping literature. Psychonomic Bulletin & Review 12:969–992.

Repp BH (2010) Sensorimotor synchronization and perception of timing: Effects of music training and task experience. Human Movement Science 29:200–213.

Rodríguez FA, Read HL, Escabí MA (2010) Spectral and Temporal Modulation Tradeoff in the Inferior Colliculus. J Neurophysiol 103:887–903.

Rogalsky C, Rong F, Saberi K, Hickok G (2011) Functional Anatomy of Language and Music Perception: Temporal and Structural Factors Investigated Using Functional Magnetic Resonance Imaging. Journal of Neuroscience 31:3843–3852.

Rutkowski RG, Weinberger NM (2005) Encoding of learned importance of sound by magnitude of representational area in primary auditory cortex. Proceedings of the National Academy of Sciences of the United States of America 102:13664–13669.

Saari P, Burunat I, Brattico E, Toiviainen P (2018) Decoding Musical Training from Dynamic Processing of Musical Features in the Brain. Scientific Reports 8.

Salimpoor VN, Benovoy M, Larcher K, Dagher A, Zatorre RJ (2011) Anatomically distinct dopamine release during anticipation and experience of peak emotion to music. Nature Neuroscience 14:257–264.

Salimpoor VN, Van Den Bosch I, Kovacevic N, McIntosh AR, Dagher A, Zatorre RJ (2013) Interactions between the nucleus accumbens and auditory cortices predict music reward value. Science 340:216–219.

Santoro R, Moerel M, De Martino F, Goebel R, Ugurbil K, Yacoub E, Formisano E (2014) Encoding of Natural Sounds at Multiple Spectral and Temporal Resolutions in the Human Auditory Cortex. PLoS Computational Biology 10.

Saxe R, Brett M, Kanwisher N (2006) Divide and conquer: A defense of functional localizers. NeuroImage 30:1088–1096.

Schneider P, Scherg M, Dosch HG, Specht HJ, Gutschalk A, Rupp A (2002) Morphology of Heschl's gyrus reflects enhanced activation in the auditory cortex of musicians. Nature Neuroscience 5:688–694.

Schneider P, Sluming V, Roberts N, Scherg M, Goebel R, Specht HJ, Dosch HG, Bleeck S, Stippich C, Rupp A (2005) Structural and functional asymmetry of lateral Heschl's gyrus reflects pitch perception preference. Nature Neuroscience 8:1241–1247.

Schönwiesner M, Zatorre RJ (2009) Spectro-temporal modulation transfer function of single voxels in the human auditory cortex measured with high-resolution fMRI. Proceedings of the National Academy of Sciences 106:14611-.

Scott SK, Blank CC, Rosen S, Wise RJS (2000) Identification of a pathway for intelligible speech in the left temporal lobe. Brain 123:2400–2406.

Shahin A, Bosnyak DJ, Trainor LJ, Roberts LE (2003) Enhancement of neuroplastic P2 and N1c auditory evoked potentials in musicians. The Journal of Neuroscience 23:5545–5552.

Singh NC, Theunissen FE (2003) Modulation spectra of natural sounds and ethological theories of auditory processing. Citation: The Journal of the Acoustical Society of America 114:3394.

Spiegel MF, Watson CS (1984) Performance on frequency-discrimination tasks by musicians and nonmusicians. Journal of the Acoustical Society of America 76:1690–1695.

Strait DL, Kraus N (2011) Can You Hear Me Now? Musical Training Shapes Functional Brain Networks for Selective Auditory Attention and Hearing Speech in Noise. Frontiers in psychology 2:10.

Teki S, Kumar S, von Kriegstein K, Stewart L, Rebecca Lyness C, Moore BCJ, Capleton B, Griffiths TD (2012) Navigating the auditory scene: An expert role for the hippocampus. Journal of Neuroscience 32:12251–12257.

Temperley D (2008) A probabilistic model of melody perception. Cognitive Science 32:418–444.

Tierney A, Dick F, Deutsch D, Sereno M (2013) Speech versus Song: Multiple Pitch-Sensitive Areas Revealed by a Naturally Occurring Musical Illusion. Cerebral Cortex 23:249–254.

Tillmann B (2005) Implicit investigations of tonal knowledge in nonmusician listeners. Annals of the New York Academy of Sciences 1060:100–110.

Tillmann B, Bigand E, Bharucha JJ (2000) Implicit Learning of Tonality: A Self-Organizing Approach. Psychological Review 107:885–913.

Trehub SE (2003) The developmental origins of musicality. Nature Neuroscience 6:669–673.

Wong PCM, Skoe E, Russo NM, Dees T, Kraus N (2007) Musical experience shapes human brainstem encoding of linguistic pitch patterns. Nature Neuroscience 10:420–422.

Zuk NJ, Teoh ES, Lalor EC (2020) EEG-based classification of natural sounds reveals specialized responses to speech and music. NeuroImage 210.

SUPPLEMENTAL FIGURES

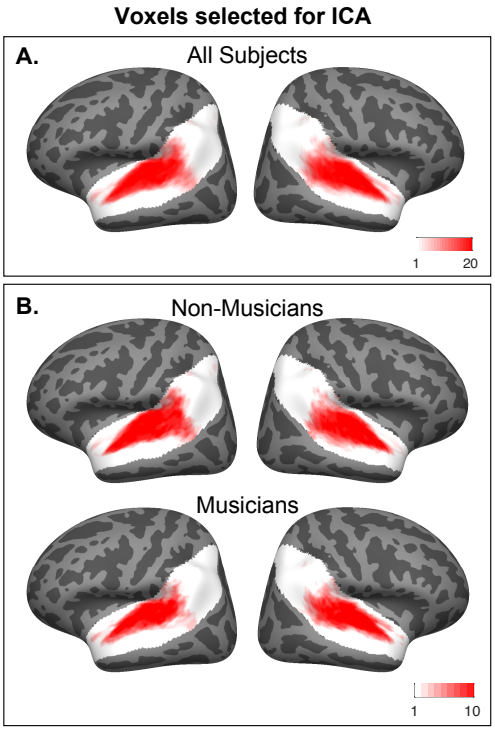

Supplemental Figure 1. Subject overlap maps showing which voxels were selected in individual subjects to serve as input to the voxel decomposition algorithm. To be selected, a voxel must display a significant ($p < 0.001$, uncorrected) response to sound (pooling over all sounds compared to silence), and produce a reliable response pattern to the stimuli across scanning sessions (see equations in Methods section). The white area shows the anatomical constraint regions from which voxels were selected. (**A**) Overlap map for all twenty subjects. (**B**) Overlap maps for non-musicians and musicians separately, illustrating that the anatomical location of the selected voxels was largely similar across groups.

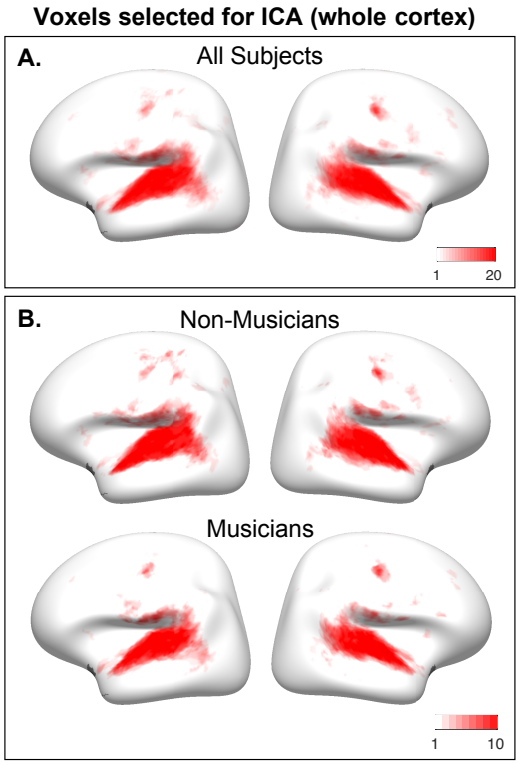

Supplemental Figure 2. Subject overlap maps showing which voxels pass the selection criteria as described in **Supplemental Figure 1**, but without any anatomical mask applied before selecting voxels.

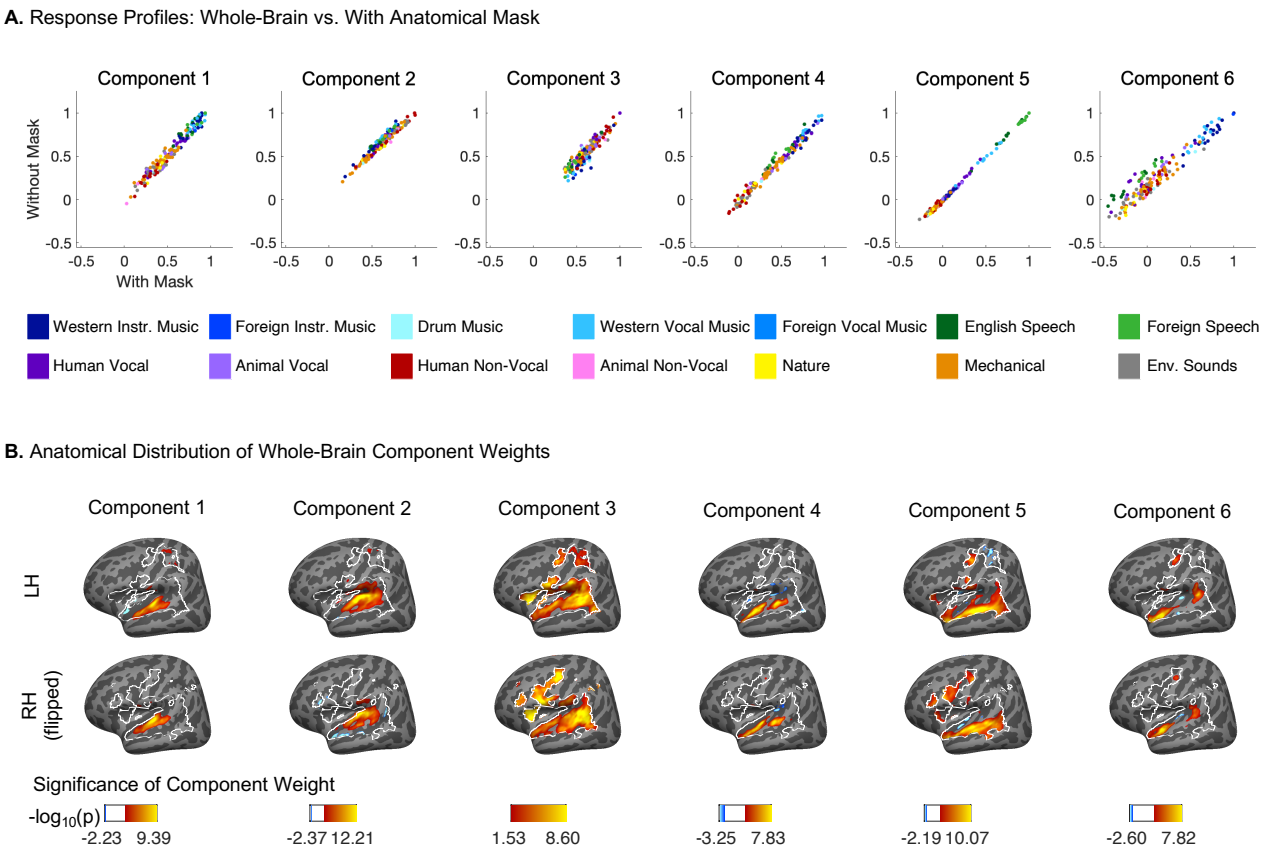

Supplemental Figure 3. **Similarity between components with anatomical mask vs. whole-brain.** (**A**) Scatter plots showing the components inferred from all 20 participants, using the voxel decomposition algorithm both with and without the anatomical mask shown in **Supplemental Figure 1**. Individual sounds are colored according to their semantic category. (**B**) Spatial distribution of whole-brain component voxel weights, computed using a random effects analysis of participants' individual component weights. Weights are compared against 0; p values are logarithmically transformed ($-\log_{10}[p]$). The white outline indicates the voxels that were both sound-responsive (sound vs. silence, $p < 0.001$ uncorrected) and split-half reliable ($r > 0.3$) at the group level. The color scale represents voxels that are significant at FDR $q = 0.05$, with this threshold being computed for each component separately. Voxels that do not survive FDR correction are not colored, and these values appear as white on the color bar. The right hemisphere (bottom row) is flipped to make it easier to visually compare weight distributions across hemispheres.

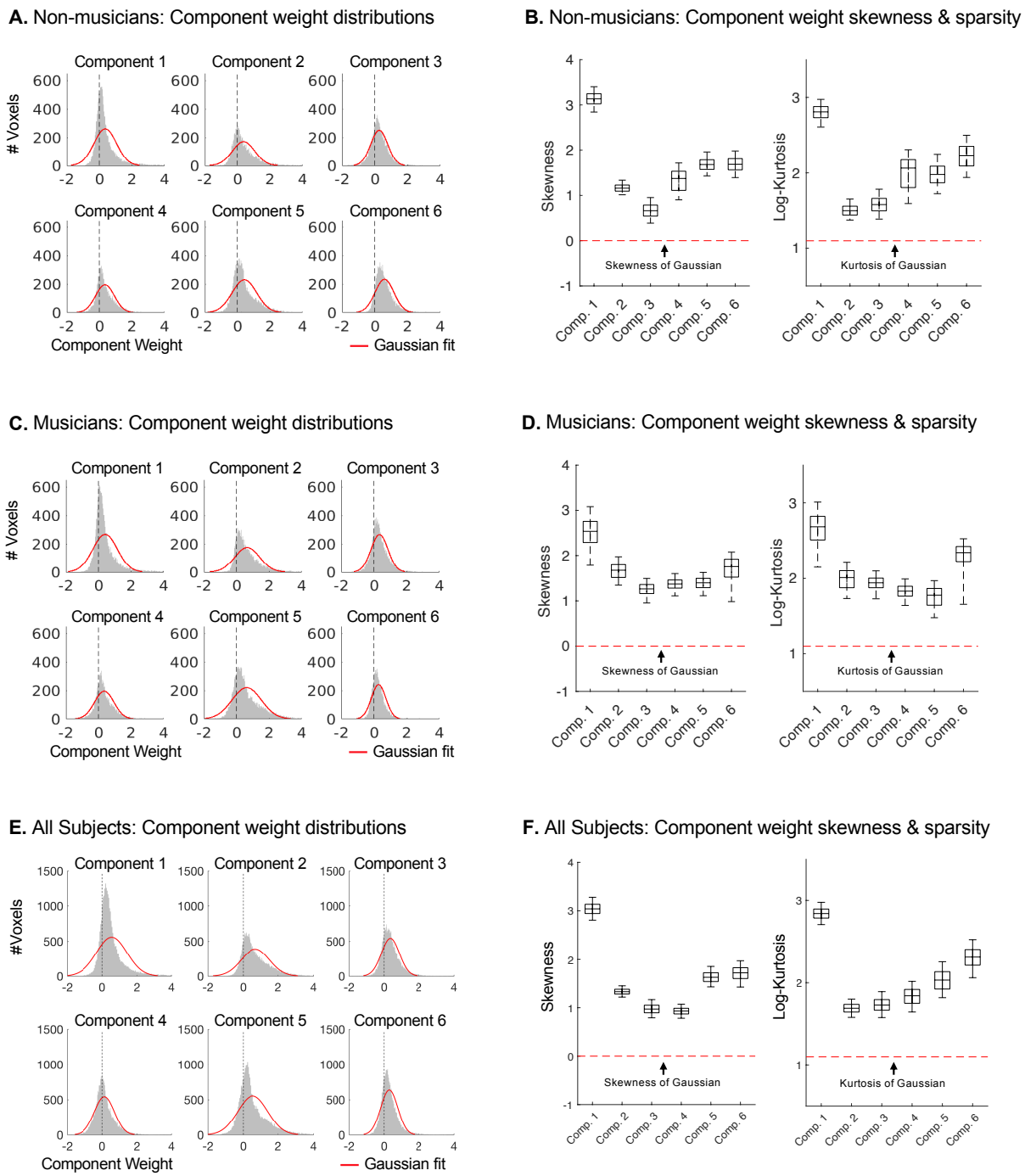

Supplemental Figure 4. Like ICA, the voxel decomposition method searches amongst the many possible solutions to the factorization problem for components that have a maximally non-Gaussian distribution of weights across voxels. (**A**) Histograms showing the weight distributions for each component inferred from non-musicians (n = 10) can be seen here, along with their Gaussian fits (red). (**B**) Skewness and log-kurtosis (a measure of sparsity) for each component inferred from musicians (n = 10), illustrating that the inferred components are skewed and sparse compared to a Gaussian (red dotted lines). Box-and-whisker plots show central 50% (boxes) and central 95% (whiskers) of the distribution for each statistic (via bootstrapping across subjects). For both the weight distribution histograms and analyses of non-Gaussianity, we used independent data to infer components (runs 1-24) and to measure the statistical properties of the component weights (runs 25-48). (**C, D**) Same as **A&B**, but for the components inferred from musicians (n = 10). (**E, F**) Same as **A&B**, but for the components inferred from all 20 participants

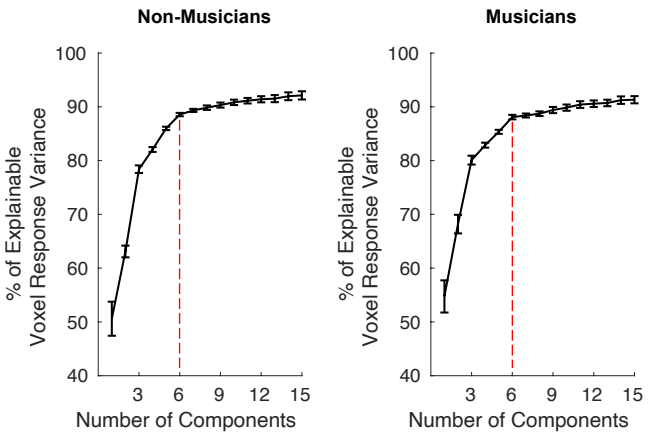

Supplemental Figure 5. The proportion of voxel response variance explained by different numbers of components, for both non-musicians (left) and musicians (right). The figure plots the median variance explained across voxels (noise corrected by split-half reliability), calculated separately for each subject and then averaged across the ten subjects in each group. Error bars plot one standard error of the mean across subjects. For both groups, 6 components were sufficient to explain over 88% of the noise-corrected variance.

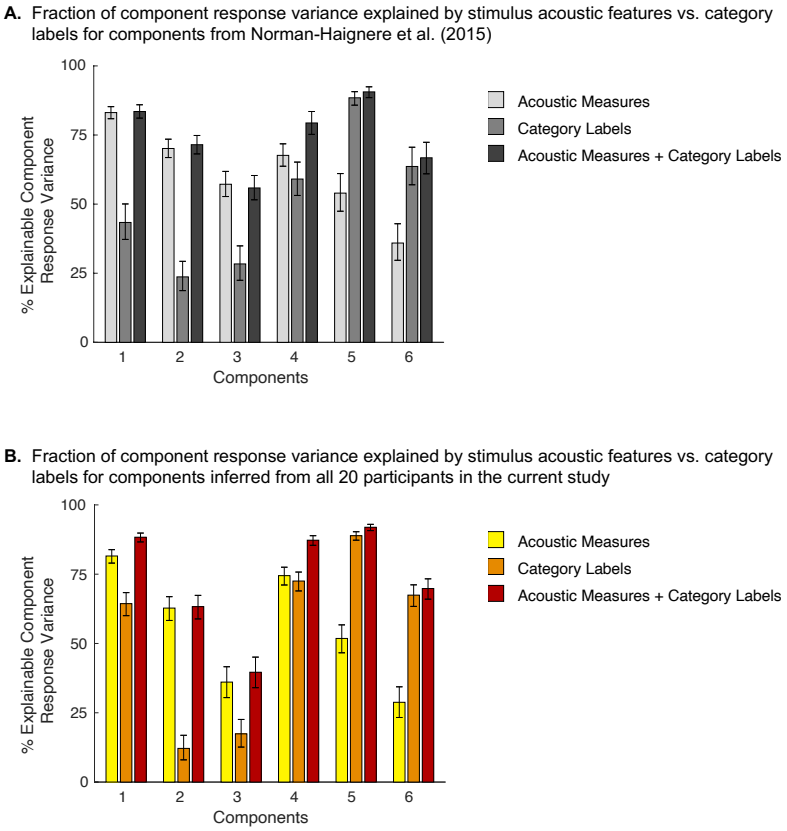

Supplemental Figure 6. Total amount of component response variation explained by (1) all acoustic measures (frequency content and spectrotemporal modulation energy), (2) all category labels (as assigned by Amazon Mechanical Turk workers), and (3) the combination of acoustic measures and category labels. (**A**) Results for components from previous study (Norman-Haignere et al., 2015). For components 1–4, category labels explained little additional variance beyond that explained by acoustic features. For Components 5 (speech-selective) and 6 (music-selective), category labels explained most of the response variance, and acoustic features accounted for little additional variance. (**B**) Same as **A** but for the components inferred from all 20 participants in the current study.

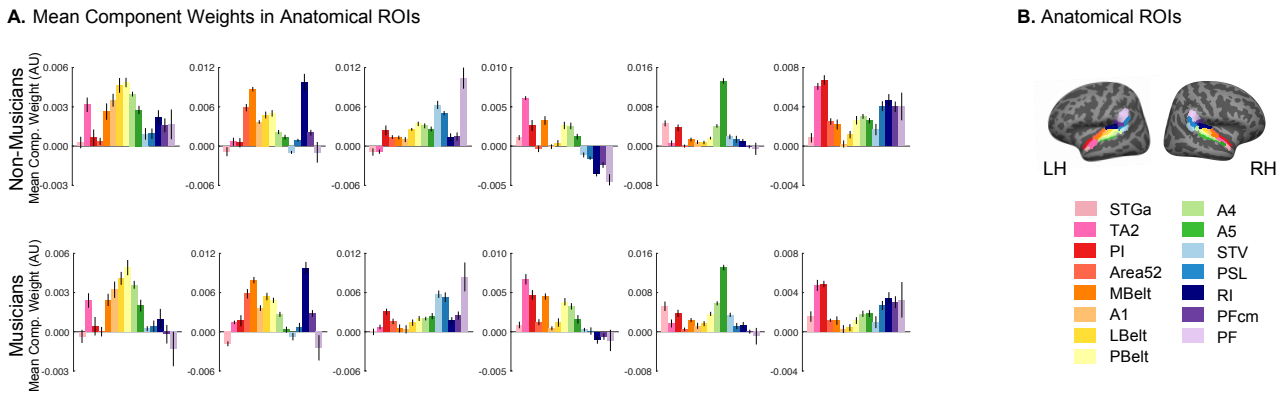

Supplemental Figure 7. Mean component voxel weights within standardized anatomical parcels (**A**) Mean component weight in a set of fifteen anatomical parcels from Glasser et al. (2016), plotted separately for non-musicians (top) and musicians (bottom). Error bars plot one standard error of the mean across participants. (**B**) Selected anatomical parcels from Glasser et al. (2016), chosen to fully encompass the superior temporal plane and superior temporal gyrus (STG).

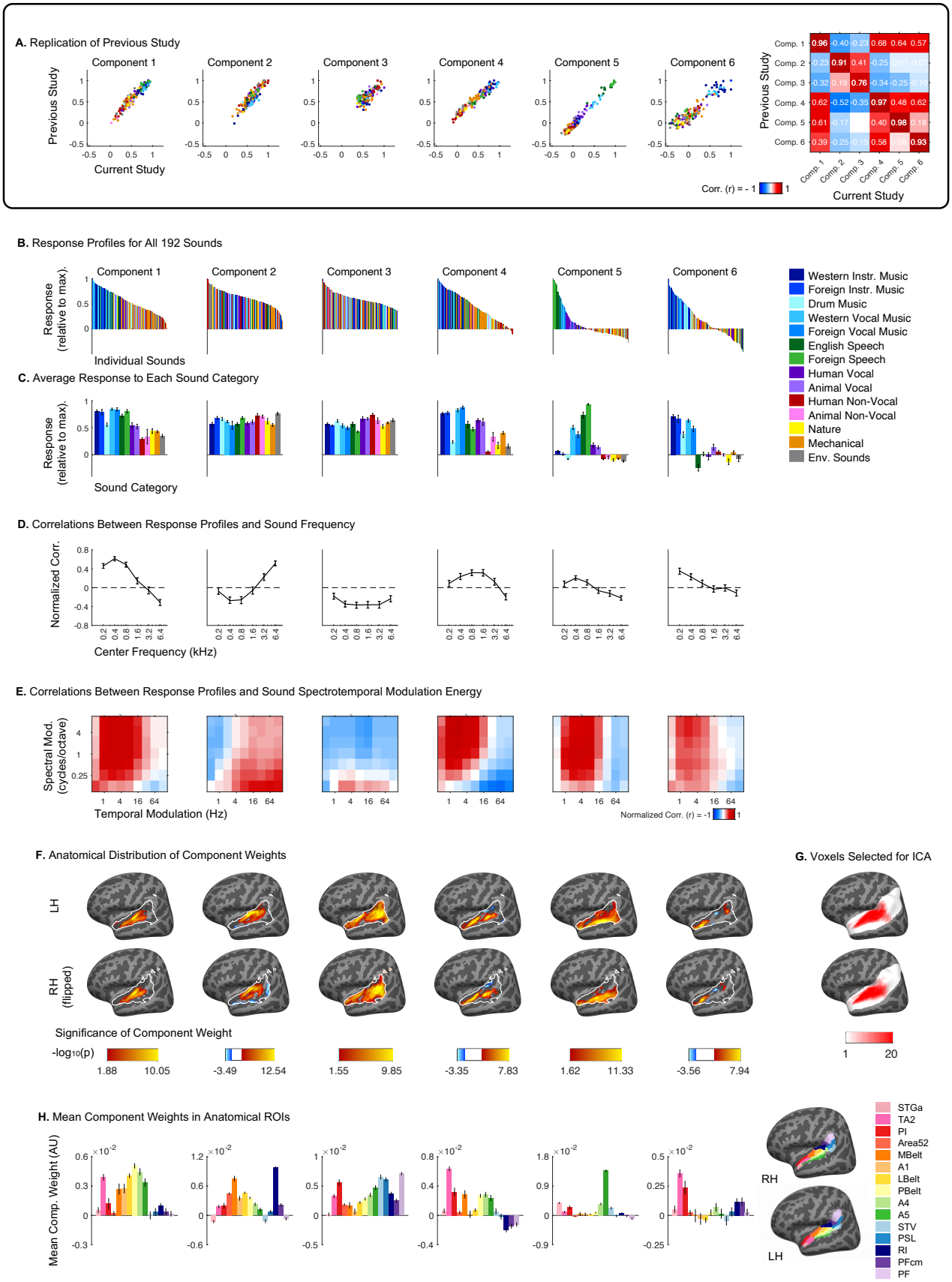
A. Replication of Previous Study
Component 1
Component 2
Component 3
Component 4
Component 5
Component 6
Previous Study
Current Study
Corr. (r) = - 1
1
B. Response Profiles for All 192 Sounds
Response (relative to max).
Individual Sounds
C. Average Response to Each Sound Category
Sound Category
Western Instr. Music
Foreign Instr. Music
Drum Music
Western Vocal Music
Foreign Vocal Music
English Speech
Foreign Speech
Human Vocal
Animal Vocal
Human Non-Vocal
Animal Non-Vocal
Nature
Mechanical
Env. Sounds
D. Correlations Between Response Profiles and Sound Frequency
Normalized Corr.
Center Frequency (kHz)
E. Correlations Between Response Profiles and Sound Spectrotemporal Modulation Energy
Spectral Mod. (cycles/octave)
Temporal Modulation (Hz)
Normalized Corr. (r) = -1
1
F. Anatomical Distribution of Component Weights
G. Voxels Selected for ICA
LH
RH (flipped)
Significance of Component Weight
-log10(p)
1.88
10.05
-3.49
12.54
1.55
9.85
-3.35
7.83
1.62
11.33
-3.56
7.94
1
20
H. Mean Component Weights in Anatomical ROIs
Mean Comp. Weight (AU)
RH
LH
STGa
TA2
PI
Area52
MBelt
A1
LBelt
PBelt
A4
A5
STV
PSL
RI
PFcm
PF

Supplemental Figure 8. Independent components inferred from voxel decomposition of auditory cortex of all 20 participants (as compared to the components in **Figures 2-5**, which were inferred from musicians and non-musicians separately). Additional plots are included here to show the extent of the replication of the results of Norman-Haignere et al. (2015). (**A**) Scatterplots showing the correspondence between the components from our previous study (y-axis) and those from the current study (x-axis). Only the 165 sounds that were common between the two studies are plotted. Sounds are colored according to their semantic category, as determined by raters on Amazon Mechanical Turk. (**B**) Response profiles of components inferred from all participants (n = 20), showing the full distribution of all 192 sounds. Sounds are colored according to their category. Note that "Western Vocal Music" stimuli were sung in English. (**C**) The same response profiles as above, but showing the average response to each sound category. Error bars plot one standard error of the mean across sounds from a category, computed using bootstrapping (10,000 samples). (**D**) Correlation of component response profiles with stimulus energy in different frequency bands. (**E**) Correlation of component response profiles with spectrotemporal modulation energy in the cochleograms for each sound. (**F**) Spatial distribution of component voxel weights, computed using a random effects analysis of participants' individual component weights. Weights are compared against 0; p values are logarithmically transformed ($-\log_{10}[p]$). The white outline indicates the 2,249 voxels that were both sound-responsive (sound vs. silence, $p < 0.001$ uncorrected) and split-half reliable ($r > 0.3$) at the group level. The color scale represents voxels that are significant at FDR $q = 0.05$, with this threshold being computed for each component separately. Voxels that do not survive FDR correction are not colored, and these values appear as white on the color bar. The right hemisphere (bottom row) is flipped to make it easier to visually compare weight distributions across hemispheres. (**G**) Subject overlap maps showing which voxels were selected in individual subjects to serve as input to the voxel decomposition algorithm (same as **Supplemental Figure 1A**). To be selected, a voxel must display a significant ($p < 0.001$, uncorrected) response to sound (pooling over all sounds compared to silence), and produce a reliable response pattern to the stimuli across scanning sessions (see equations in Methods section). The white area shows the anatomical constraint regions from which voxels were selected. (**H**) Mean component voxel weights within standardized anatomical parcels from Glasser et al. (2016), chosen to fully encompass the superior temporal plane and superior temporal gyrus (STG). Error bars plot one standard error of the mean across participants.

SUPPLEMENTAL INFORMATION

Behavioral data acquisition & analysis

To validate participants' self-reported musicianship, we measured participants' abilities on a variety of psychoacoustical tasks for which prior evidence suggested that musicians would outperform non-musicians. For all psychoacoustic tasks, stimuli were presented using Psychtoolbox for Matlab (Brainard, 1997). Sounds were presented to participants at 70dB SPL over circumaural Sennheiser HD280 headphones in a soundproof booth (Industrial Acoustics) (SPL level was computed without any weighting across time or frequency). After each trial, participants were given feedback about whether or not they had answered correctly. Group differences for each task were measured using non-parametric Wilcoxon rank sum tests.

Pure tone frequency discrimination. Because musicians have superior frequency discrimination abilities when compared to non-musicians (Spiegel and Watson, 1984; Kishon-Rabin et al., 2001; Micheyl et al., 2006), we first measured participants' pure tone frequency discrimination thresholds using an adaptive two-alternative forced choice (2AFC) task. In each trial, participants heard two pairs of tones. One of the tone pairs consisted of two identical 1 kHz tones, while the other tone pair contained a 1 kHz tone and a second tone of a different frequency. Participants determined which tone interval contained the frequency change. The magnitude of the frequency difference was varied adaptively using a 1-up 3-down procedure (Levitt, 1971), which targets participants' 79.4% threshold. The frequency difference was changed initially by a factor of two, which was reduced to a factor of $\sqrt{2}$ after the fourth reversal. Once 10 reversals had been measured, participants' thresholds were estimated as the average of these 10 values. Multiple threshold estimations were obtained per participant (3 threshold estimations for the first seven participants, and 5 for the remaining 13 participants), and then averaged.

Synchronized tapping to an isochronous beat. Sensorimotor abilities are crucial to musicianship, and finger tapping tasks show some of the most reliable effects of musicianship (Repp, 2005, 2010; Bailey and Penhune, 2010). Participants were asked to tap along with an isochronous click track. They heard ten 30-second click blocks, separated by 5 seconds of silence. The blocks varied widely in tempo, with interstimulus intervals ranging from 200ms to 1 second (tempos of 60 to 300 bpm). Each tempo was presented twice, and the order of tempi was permuted across participants. We recorded the timing of participants' responses using a tapping sensor we constructed and have used in previous studies (Jacoby and McDermott, 2017; Polak et al., 2018). We then calculated the difference between participants' response onsets and the actual stimulus onsets. The standard deviation of these asynchronies between corresponding stimulus and response onsets was used as a measure of sensorimotor synchronization ability (Polak et al., 2018).

Melody discrimination. Musicians have also been reported to outperform non-musicians on measures of melodic contour and interval discrimination (Fujioka et al., 2004; McDermott et al., 2010; McPherson and McDermott, 2018). In each trial, participants heard two five-note melodies, and were asked to judge whether the two melodies were the same or different. Melodies were composed of notes that were randomly drawn from a log uniform distribution of semitone steps from 150Hz to 270Hz. The second melody was transposed up by half an octave and was either identical to the first melody or contained a single note had that had been altered either up or down by 1 or 2 semitones. Half of the trials contained a second melody that was the same as the first melody, while 25% contained a pitch change that preserved the melodic contour and the remaining 25% contained a pitch change that violated the melodic contour. There were 20 trials per condition (same/different melody x same/different contour x 1/2 semitone change), for a total of 160 trials. This task was modified from (McPherson and McDermott, 2018).

"Sour note" detection. To measure participants' knowledge of Western music, we also measured participants' ability to determine whether a melody conforms to the rules of Western music theory. The melodies used in this experiment were randomly generated from a probabilistic generative model of Western tonal melodies that creates a melody on a note-by-note basis according to the principles that (1) melodies tend to be limited to a narrow pitch range, (2) note-to-note intervals tend to be small, and (3) the notes within the melody conform to a single key (Temperley, 2008). In each trial of this task, participants heard a 16-note melody and were asked to determine whether the melody contained an out-of-key ("sour") note. In half of the trials, one of the notes in the melody was modified so that it was rendered out of key. The modified notes were always scale degrees 1, 3, or 5 and they were modified by either 1 or 2 semitones accordingly so that they were out of key (i.e. scale degrees 1 and 5 were modified by 1 semitone, and scale degree 3 was modified by 2 semitones). Participants judged whether the melody contained a sour note (explained as a "mistake in the melody"). There were 20 trials per condition (modified or not x 3 scale degrees), for a total of 120 trials. This task was modified from (McPherson and McDermott, 2018).

Psychoacoustic results

As predicted, musicians outperformed non-musicians on all behavioral psychoacoustic tasks, replicating prior findings (**Supplemental Figure 9**). Consistent with previous reports (Spiegel and Watson, 1984; Kishon-Rabin et al., 2001; Micheyl et al., 2006), musicians performed slightly better on the frequency discrimination task (median discrimination threshold = 0.51%, sd = 0.12%) than non-musicians (median discrimination threshold = 0.57%, sd = 0.23%); this difference was marginally significant ($z = -1.32$, $p = 0.09$, effect size $r = -0.30$, one-tailed Wilcoxon rank sum test, **Supplemental Figure 9A**). Musicians were also better able to synchronize their finger tapping with an isochronous beat, showing significantly less variability than non-musicians in their response (sd = 22.4ms) than non-musicians (sd = 37.7ms, $z = -2.68$, $p < 0.01$, effect size $r = -0.60$, one-tailed Wilcoxon rank sum test, **Supplemental Figure 9B**). When presented with musical melodies, musicians were better able to discriminate between two similar melodies (musician median ROC area = 0.82, sd = 0.08, non-musician mean ROC area = 0.66, sd = 0.09, $z = 3.21$, $p < 0.001$, effect size $r = 0.72$, one-tailed Wilcoxon rank sum test, **Supplemental Figure 9C**), and to detect scale violations within melodies (musician mean ROC area = 0.89, sd = 0.06, non-musicians mean ROC area = 0.70, sd = 0.10, $z = 3.44$, $p < 0.001$, effect size $r = 0.77$, one-tailed Wilcoxon rank sum test, **Supplemental Figure 9D**). These behavioral effects validate our participants' self-reported status as trained musicians or non-musicians.

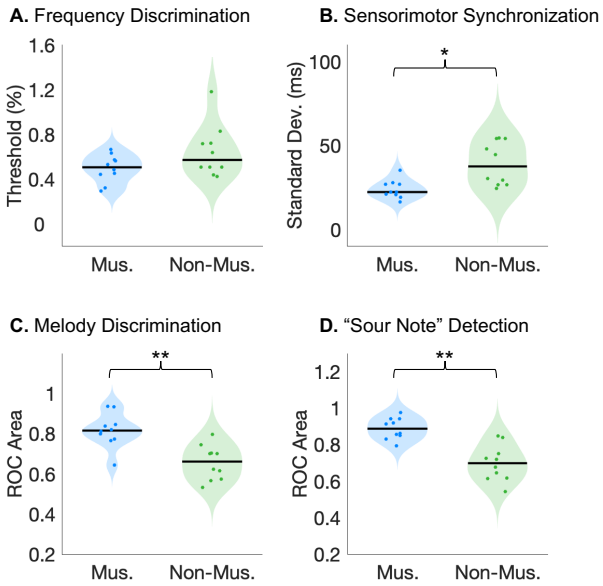

Supplemental Figure 9. Musicians outperform non-musicians on psychoacoustic tasks. (**A**) Participants' pure tone frequency discrimination thresholds were measured using a 1-up 3-down adaptive two-alternative forced choice (2AFC) task, in which participants indicated which of two pairs of tones were different in frequency. Note that lower thresholds correspond to better performance. (**B**) Sensorimotor synchronization abilities were measured by instructing participants to tap along with an isochronous beat at various tempos, and comparing the standard deviation of the difference between participants' response onsets and the actual stimulus onsets. (**C**) Melody discrimination was measured using a 2AFC task, in which participants heard two five-note melodies (with the second one transposed up by a tritone) and were asked to judge whether the two melodies were the same or different. (**D**) We measured participants' ability to determine whether a melody conforms to the rules of Western music theory by creating 16-note melodies using a probabilistic generative model of Western tonal melodies (Temperley, 2008), and instructing participants to determine whether or not the melody contained an out-of-key ("sour") note. Mus. = musicians, Non-Mus. = non-musicians. * = significant at $p < 0.01$ one-tailed, ** = significant at $p < 0.001$ one-tailed.

Replication of Norman-Haignere et al. (2015) using data from all 20 participants

In addition to conducting the voxel decomposition analysis separately for musicians and non-musicians, we were able replicate the full results from Norman-Haignere et al. (2015) using data from all 20 participants from both groups. The components from this combined analysis were used when directly comparing component weights between groups (described in Results sections titled "Music component weight magnitude differs only slightly between musicians and non-musicians" and "Similar anatomical distribution of music component weights in musicians and non-musicians"). Here, we describe that analysis in more detail, and explain more about the four components that are selective for acoustic stimulus features.

In our previous study (Norman-Haignere et al., 2015), prior to applying the voxel decomposition algorithm, each participant's responses were de-meaned across voxels, such that each participant had the same mean response (across voxels) for a given sound. This normalization was included to prevent the voxel decomposition algorithm from discovering additional components that were driven by a single participant (e.g. due to non-replicable sources of noise, such as motion during a scan). However, this analysis step would also remove any group difference in the average response to certain sounds (e.g. music stimuli). To prevent this effect from influencing the comparison of the two groups, we ran the voxel decomposition algorithm without demeaning by individual participants. As expected, this resulted in a larger number of components, with 8 components being needed to optimally model the data from all 20 participants, explaining 89.83% of the voxel response variance, after which the amount of explained variance for each additional component plateaued.

Of the 8 components derived from the non-demeaned data, six of them were each very similar to one of the 6 components from Norman-Haignere et al. (2015) and accounted for 87.54% of voxel response variance. Because the components inferred using ICA have no order, we first used the Hungarian algorithm (Kuhn, 1955) to optimally reorder the components, maximizing their correlation with the components from our previous study. As expected, the reordered components were highly correlated, with r-values ranging from 0.76 to 0.98 (**Supplemental Figure 8A**; see **Supplemental Figure 8B** for the response profiles of the components, and **Supplemental Figure 8C** for the profiles averaged within sound categories). To confirm that these strong correlations are not simply an artifact of the Hungarian algorithm matching procedure, we ran a permutation test in which we re-ordered the sounds within each component 1,000 times, each time using the Hungarian algorithm to match these permuted components with those from our previous study. The resulting correlations between the original components their corresponding permuted components were very low (mean r-values ranging from 0.086 to 0.098), with the maximum correlation over all 1,000 permutations not exceeding r = 0.3 for any component.

The additional two components were much less correlated with any of the six original components, with the strongest correlation being r = 0.28. As expected, the weights of these additional two components were concentrated in a small number of participants (one almost entirely loading onto a single non-musician participant, and the other onto a small group comprised of both musicians and non-musicians). For this reason, we omitted these two components from further analyses and focused on the set of six components that closely match those discussed previously (**Supplemental Figure 8B-H**). The non-Gaussianity of these 6 components can be seen in **Supplemental Figure 4A** (skewness ranging from 1.06 to 2.96, log-kurtosis ranging from 1.70 to 2.79).

As in Norman-Haignere et al. (2015), four of the components were selective for different acoustic properties of sound (**Supplemental Figure 8D** & **E**), while two components were selective for speech (component 5) and music respectively (component 6) (**Supplemental Figure 8B** & **C)**. The components replicated all of the functional and anatomical properties from our prior study, which we briefly describe here.

Components 1 and 2 exhibited high correlations between their response profiles and measures of stimulus energy in either low (component 1) or high frequency bands (component 2) (**Supplemental Figure 8D**). The group anatomical weights for components 1 and 2 concentrated in the low and high-frequency regions of primary auditory cortex (**Supplemental Figure 8F** & **H**) (Rauschecker et al., 1995; Humphries et al., 2010; Da Costa et al., 2011; Baumann et al., 2013). We did not measure tonotopy in the individual participants from this study, but our previous study did so, and found a close correspondence between individual participant tonotopic maps and the weights for these two components. Components also showed tuning to spectrotemporal modulations (**Supplemental Figure 8E**), with a tradeoff between selectivity for fine spectral and slow temporal modulation (components 1 and 4) verses coarse spectral and fast temporal modulation (components 2 and 3) (Singh and Theunissen, 2003; Rodríguez et al., 2010). Component 4, which exhibited selectivity for fine spectral modulation, was concentrated anterior to Heschl's gyrus (component 4, **Supplemental Figure 8F** & **H**), similar to prior work that has identified tone-selective regions in anterolateral auditory cortex in humans (Patterson et al., 2002; Penagos et al., 2004; Norman-Haignere et al., 2013). Conversely, selectivity for coarse spectral modulation and fast temporal modulation was concentrated in posterior regions of auditory cortex (component 3, **Supplemental Figure 8F** & **H**) (Santoro et al., 2014), consistent with previous studies reporting selectivity for sound onsets in caudal areas of human auditory cortex (Hamilton et al., 2018).

The two remaining components responded selectively to speech and music, respectively (component 5 and 6, **Supplemental Figure 8C**), and were not well accounted for using acoustic properties alone (**Supplemental Figure 8B**). The weights for the speech-selective component (component 5) were concentrated in the middle portion of the superior temporal gyrus (midSTG, **Supplemental Figure 8F** & **H**), as expected (Scott et al., 2000; Hickok and Poeppel, 2007; Overath et al., 2015). In contrast, the weights for the music-selective component (component 6) were most prominent anterior to PAC in the planum polare, with a secondary cluster posterior to PAC in the planum temporale (**Supplemental Figure 8F** & **H**) (Ohnishi et al., 2001; Margulis et al., 2009; Dick et al., 2011; Fedorenko et al., 2012; Angulo-Perkins et al., 2014; Armony et al., 2015; Norman-Haignere et al., 2015).

These results closely replicate the functional organization of human auditory cortex reported by Norman-Haignere et al. (2015), including the existence and anatomical location of inferred music-selective neural populations.